Title
The kinase Isr1 negatively regulates hexosamine biosynthesis in S. cerevisiae

Author
Alme, Emma Bette

Publication Date
2020

Peer reviewed|Thesis/dissertation

The kinase Isr1 negatively regulates hexosamine biosynthesis in S. cerevisiae

by
Emma B Alme

DISSERTATION
Submitted in partial satisfaction of the requirements for degree of
DOCTOR OF PHILOSOPHY

in

Biochemistry and Molecular Biology

in the

GRADUATE DIVISION
of the
UNIVERSITY OF CALIFORNIA, SAN FRANCISCO

Approved:

DocuSigned by:
David Toczyski
B39DA64A208E4CB...

David Toczyski
Chair

DocuSigned by:
Alexander Johnson
[illegible]45B...

Alexander Johnson

DocuSigned by:
Dyche Mullins
E4FB70A20A7546F...

Dyche Mullins

Committee Members

Acknowledgements

I would like to thank my friends, family, colleagues, and mentors, all of whom contributed to this dissertation by supporting me throughout my PhD. First, I'd like to thank my advisor, Dave Toczyski, for always making mentorship a priority. As important as the science is to him, he cares about his students as people first, which I have always appreciated. Dave's scientific guidance was invaluable throughout my PhD. I felt like I could take any scientific problem to him –large or small, and he always had an amazing ability to know enough of what I was up to in order to be helpful without micromanaging my work. His cocktail making prowess was also very much appreciated on many any occasions. I'd also like to thank my other thesis committee members, Dyche Mullins and Sandy Johnson, both for their scientific guidance and for their support of my desire to entire a career in science policy. They both offered advice during my thesis committee meetings that was tailored to my career goals, which I very much appreciated.

While in graduate school, I discovered and pursued a passion for science policy and I am grateful to my mentors outside of the lab who have helped me turn this into my next career step. Keith Yamamoto and India Hook-Barnard provided me with an incredible amount of opportunities to explore and be a part of science policy endeavors at UCSF. They supported and helped me grow the Science Policy Group at UCSF, which was one of the most rewarding parts of graduate school for me. Thanks to India and Keith, I am writing this acknowledgement as a Christine Mirzayan Science and Technology Policy Fellow at the National Academies of Science, Medicine and Engineering. I'd also like to thank Liz Watkins and Liz Silva, both of whom always

championed student groups on campus and are always advocating for graduate students. Thank you to the members of the Science Policy Group at UCSF, particularly Steven Moss, David Paquette and Elina Kostyanovskaya, for all of their hard work and dedication.

Throughout my PhD, my labmates were an endless source of support and generously helped out on my project: In particular, Jessica Lao taught me a lot of what I know about yeast biology and never seemed to get impatient no matter how many questions I had. Fernando Meza Gutierrez and Nerea Sanvisens Delgado also shared a lot of helpful yeast biology techniques, protocols, and reagents with me. Kevin Mark first identified Isr1 in a proteomics screen in his own paper, so my project would never have started without him. Katie Ulrich, Kaili Carr, and Harold Marin were all technicians in the lab during my PhD and I would never have been able to do these experiments without their work managing our lab. Frances Hundley pulled countless plates and cultures for me, tolerated a graveyard of pipette tips on the floor around our benches, and endured years of me constantly distracting her whenever we were both at our desks. As we were in the same cohort and were experiencing the process of graduate school together, she was a constant source of support. I will always be grateful I got share my bench with her.

My PhD would never have been remotely as enjoyable without my friends and family, particularly the strong friendships I formed during my first year. I am so thankful for Bettie Osuna, Jonathan Asfaha, Terri Lee and Nathan Gamarra for their lifelong friendship. In addition to his friendship, Jonathan also provided me with countless reagents for my project and very helpful advice. I am incredibly thankful to my parents

for making it clear from an early age that graduate school was something we would all do. I know I am only where I am today because of their endless support, guidance, and love. Because of them, I have led an incredibly fortunate life and I owe them everything. I would never have even been able to conceive of this achievement without them. Thank you also to my brother for always being proud of me no matter what. And finally, thank you to my husband, Chris, who met me when I was already deep into my third year of graduate school and has been by my side ever since. Thank you for making all of life worthwhile. I love you endlessly.

Contributions

The work described in Chapter 1 has been submitted for publication in a peer reviewed journal. Emma Alme conceptualized, designed, and carried out all experiments other than the mass spectrometry described in Figure 1.4. Erica Stevenson and Danielle Swaney performed the mass spectrometry experiments, which were overseen by Danielle Swaney. Emma Alme wrote the manuscript in collaboration with David Toczyski, who oversaw the project.

Abstract

The kinase Isr1 negatively regulates hexosamine biosynthesis in *S. cerevisiae*

By Emma B. Alme

Protein phosphorylation is an essential regulatory mechanism that controls most cellular processes, integrating a variety of environmental signals to drive cellular growth. Yeast encode over 100 kinases, yet many remain poorly characterized. The *S. cerevisiae* gene *ISR1* encodes a putative kinase with no ascribed function. Here, we show that *ISR1* decreases the synthesis of a critical structural carbohydrate, uridine diphosphate N-acetylglucosamine (UDP-GlcNAc), by mediating inhibition of one of the enzymes responsible for its synthesis, Gfa1. UDP-GlcNAc is the precursor to protein glycosylation, GPI anchor formation, and chitin synthesis, the first two of which are essential and conserved in humans. Throughout the cell cycle, and in response to changing environmental conditions, the cell must balance its use of glucose for energy production and generation of these structural carbohydrates. Here we show that Isr1 is regulated by both cell cycle and nutrient changes, and is rapidly degraded in a phosphorylation dependent manner. Isr1-mediated inhibition of UDP-GlcNAc synthesis may serve as a mechanism of dynamically regulating how the cell utilizes glucose in response to its environment.

Table of Contents

List of Figures

Chapter 1

List of Tables

Chapter 1

Chapter 1

The kinase Isr1 negatively regulates hexosamine biosynthesis in *S. cerevisiae*

The kinase Isr1 negatively regulates hexosamine biosynthesis in *S. cerevisiae*

Emma B Alme[1,2], Erica Stevenson[3,4,5], Nevan J Krogan[3,4,5], Danielle L Swaney[3,4,5], David P Toczyski[1,2*]

1. Department of Biochemistry and Biophysics, University of California San Francisco, San Francisco, California, United States of America

2. Helen Diller Family Comprehensive Cancer Center, University of California San Francisco, San Francisco, California, United States of America

3. Department of Cellular and Molecular Pharmacology, University of California San Francisco, San Francisco, California, United States of America

4. California Institute for Quantitative Biosciences, University of California San Francisco, San Francisco, California, United States of America

5. J. David Gladstone Institutes, San Francisco, California, United States of America

Abstract

The *S. cerevisiae ISR1* gene encodes a putative kinase related to mammalian Raf and with no ascribed function. Here, we show that Isr1 acts as a negative regulator of the highly-conserved hexosamine biosynthesis pathway (HBP), which converts glucose into uridine diphosphate N-acetylglucosamine (UDP-GlcNAc), the carbohydrate precursor to protein glycosylation, GPI-anchor formation, and chitin biosynthesis. Overexpression of *ISR1* is lethal and, at lower levels, causes sensitivity to tunicamycin and resistance to calcofluor white, implying impaired protein glycosylation and reduced chitin deposition. Gfa1 is the first enzyme in the HBP and is conserved from bacteria and yeast to humans. The lethality caused by Isr1 overexpression is rescued by co-overexpression of *GFA1* or exogenous glucosamine, which bypasses *GFA1's* essential function. Gfa1 is phosphorylated in an *ISR1*-dependent fashion and mutation of *ISR1*-dependent sites ameliorates the lethality associated with Isr1 overexpression. Isr1 contains a phosphodegron that is phosphorylated by Pho85 and subsequently ubiquitinated by the SCF-Cdc4 complex, largely confining Isr1 protein levels to the time of bud emergence. Mutation of this phosphodegron stabilizes Isr1 and recapitulates the overexpression phenotypes. As Pho85 is a cell cycle and nutrient responsive kinase, this tight regulation of Isr1 may serve to dynamically regulate flux through the HBP and modulate how the cell's energy resources are converted into structural carbohydrates in response to changing cellular needs.

Introduction

Protein phosphorylation is a major signaling mechanism that is critical to the control of most cellular processes [1–3]. It is estimated that 75% of the proteome is phosphorylated and kinases are among the largest protein families, comprising about 2% of most eukaryotic genomes [4]. Kinases often act in cascades to amplify signals and there is significant cross-talk amongst protein kinases, allowing for the coordination of many cellular inputs. Despite their abundance and critical regulatory roles in the cell, many of the approximately 130 yeast kinases remain poorly characterized [5].

One such kinase is Inhibitor of Staurosporine Resistance 1 (Isr1), which is annotated as a putative kinase based on homology of its kinase domain to Raf [6]. Raf kinase is a MAPKK best known for its oncogenic functions downstream of RAS in humans [7]. In *S. cerevisiae,* no Raf homologue has been identified and RAS functions primarily upstream of adenylyl cyclase in response to nutrient levels [8]. The Isr1 kinase domain shares 24% identity and 43% similarity to Byr2, the Raf homologue in *S. pombe.* However, while Byr2 binds to and is directly activated by RAS, Isr1 does not appear to be downstream of RAS [9,10].

ISR1 was first identified as a gene whose deletion is synthetic lethal with a temperature-sensitive allele of *PKC1* and whose overexpression sensitized cells to staurosporine, a Pkc1 inhibitor [6]. While the molecular basis for these phenotypes was unknown, they suggested a defect in cell wall homeostasis. Pkc1 is essential to the cell wall integrity pathway, which is critical to remodeling the cell wall in response to cellular growth and environmental stress [11]. Other studies identified *ISR1* as a gene whose overexpression causes sensitivity to caffeine, a general cell wall stress agent, and

resistance to zymocin [12]. As chitin is the cellular receptor for zymocin [13], these phenotypes are consistent with reduced levels of chitin, a minor but critical structural component of the cell wall, comprising approximately 2% of the cell wall by mass [14]. The major protein component of the cell wall is glycosylphosphatidylinositol (GPI) anchors. Both GPI anchors and chitin share the same carbohydrate precursor, uridine diphosphate N-acetylglucosamine (UDP-GlcNAc), which is also the precursor for protein glycosylation [14]. Many proteins involved in cell wall carbohydrate biosynthesis are heavily glycosylated, making regulated production of this carbohydrate essential for proper cell wall homeostasis. N-glycosylation is also critical to many other cellular processes, including proper protein folding and trafficking as well as cell cycle progression [14,15]. The cellular requirement for UDP-GlcNAc changes throughout the cell cycle. While protein glycosylation occurs continuously as a cell grows, chitin synthesis predominates in G1 at the time of bud emergence and chitin deposition also greatly increases in response to cell wall stress [16–20].

UDP-GlcNAc is synthesized via the hexosamine biosynthesis pathway (HBP), which is highly conserved from bacteria to humans [21]. Most of the glucose imported into the cell is shunted into glycolysis after it is converted to fructose-6-phosphate, but approximately 6% enters the hexosamine biosynthesis pathway where it is converted into UDP-GlcNAc though the sequential action of four enzymes: glutamine: fructose-6-phosphate aminotransferase (Gfa1), GlcN-6-P acetyltransferase (Gna1), Phosphoacetyl-glucosamine mutase (Pcm1) and UDP-GlcNAc pyrophosphorylase (Qri1) [22]. The first step of this pathway, conversion of fructose-6-phosphate and glutamine to glucosamine-6-phosphate, is mediated by Gfa1 and is the rate limiting step

of the pathway [17,21]. Gfa1 activity has been shown to be directly proportional to UDP-GlcNAc synthesis and is regulated by nutrient and stress-responsive kinases (23–27).

We have identified a role for Isr1 as an inhibitor of the HBP, establishing a function for this kinase. High levels of Isr1 promotes Gfa1 phosphorylation, and inhibition of the HBP by Isr1 is relieved by mutation of these Gfa1 phosphosites or bypassing Gfa1 by exogenous addition of glucosamine. Additionally, we have identified a critical Pho85-regulated SCF^{CDC4} phosphodegron in *ISR1.* Mutation of this phosphodegron strongly affects HBP activity, highlighting how strict control of this kinase by post-translational modification can allow for signal integration and tight regulation of the HBP in response to changing cellular stimuli.

Results

Overexpression of Isr1 kinase activity is lethal

To begin to understand the role Isr1 might play in the cell, we first sought to test the effect of overexpressing *ISR1*. We placed the *ISR1* ORF under the control of the *GAL1* promoter on a 2μ plasmid. At this level of expression (referred to as GAL-2μ), Isr1 is lethal to the cell (Fig 1.1.1A). Isr1 is a putative kinase and mutation of the predicted aspartic acid proton acceptor in its kinase domain to alanine abolished this lethality, indicating that kinase activity is required for Isr1 function (Fig 1.1A). Isr1 is a very low abundant protein [28] and difficult to overexpress for reasons that are currently unknown. The expression level of Isr1 from a 2μ plasmid utilizing the *ISR1* promoter (referred to as 2μ *ISR1*) is low compared to GAL-2μ *ISR1,* and even GAL-2μ *ISR1* does not result in extremely high levels of Isr1 (Fig 1.1B). To determine the levels of Isr1 achieved by this construct, we epitope tagged Pkc1 expressed under its endogenous promoter using a 3x-Flag tag, the same epitope tag used for Isr1. Based on comparison of these proteins by western blot, GAL-2μ Isr1 protein levels are similar to the endogenous expression level of Pkc1 (Fig 1.1C).

Isr1 does not function in RNA processing

In contrast to the lethality we saw with GAL-2μ *ISR1*, in large scale studies using the *MATa* deletion collection, deletion of *ISR1* has resulted in few phenotypes [29]. *ISR1* deletion was shown to result in sensitivity to cordycepin, an adenosine analogue that causes premature termination, indicating a role in RNA processing [30]. However, we found that while the *isr1Δ::KanMX* strain isolated from the *MATa* deletion collection

did show sensitivity to cordycepin (Fig 1.2A), this was not rescued by integrating *ISR1* at the endogenous locus in this strain. By contrast, we observed that *isr1*Δ was resistant to tunicamycin, an N-glycosylation inhibitor [31]. This phenotype was not previously reported and sensitivity to tunicamycin was restored by integrating *ISR1* in the *isr1*Δ strain (Fig 1.2A). This indicates that tunicamycin resistance, but not cordycepin sensitivity, is dependent on Isr1 activity. The 3'UTR of *ISR1* overlaps with that of its neighboring gene, *YTH1*, which is an essential component of the mRNA cleavage and polyadenylation factor. Thus, the cordycepin sensitivity of the *isr1*Δ strain from the deletion collection is likely a result of a reduction in function of *YTH1*. Importantly, many of the genetic interactions reported for *ISR1* from large scale studies using the *MATa* deletion collection are likely due to this neighboring gene effect as well, making it difficult to discern which phenotypes are specific to *ISR1*. This caveat of large scale collections has been previously described and the neighboring gene effect is estimated to result in incorrect annotation of approximately 10% of genes [32]. We generated our own *isr1*Δ strain using a hygromycin selectable marker and found that this strain did not exhibit sensitivity to cordycepin, but did show resistance to tunicamycin (Fig 1.2A). This *isr1*Δ*::HygMX* strain is used in all subsequent experiments.

Isr1 overexpression has phenotypes associated with a deficiency in UDP-GlcNAc

Given the resistance to tunicamycin that we uncovered with our newly generated *isr1*Δ strain, we wished to determine if higher levels of *ISR1,* reciprocally*,* caused tunicamycin sensitivity. Because of the lethality associated with GAL-2μ *ISR1*, we performed this characterization utilizing 2μ *ISR1*. We added a NAT selectable marker to the plasmid to

allow drug screening on rich media containing NAT instead of synthetic dropout media, allowing for lower concentrations of drugs to be used. 2μ overexpression of *ISR1*, but not a kinase dead allele, *isr1-D280A*, resulted in sensitivity to tunicamycin (Fig 1.2B). Tunicamycin acts as an ER-stress agent by inhibiting the first step in N-glycosylation, which involves the transfer of N-acetylglucosamine-1-phosphate (GlcNAc-1-P) from UDP-N-acetylglucosamine (UDP-GlcNAc) to the carrier lipid dolichyl-phosphate (Dol-P) [31,33]. Thus, the sensitivity to tunicamycin in response to Isr1 overexpression could be due to a defect in N-glycosylation or a general increase in ER-stress. To distinguish between these possibilities, we tested if *ISR1* overexpression conferred sensitivity to other ER stress agents and found that GAL-2μ *ISR1* did not confer sensitivity to DTT, suggesting that the tunicamycin sensitivity is not due to a general increase in ER-stress (Fig 1.2C). For reasons that are currently unknown, the GAL-2μ *ISR1* phenotype is less severe on synthetic media, allowing this sensitivity test to be performed.

We also found that 2μ *ISR1* conferred resistance to calcofluor white (Fig 1.2B), recapitulating previous data indicating a role for *ISR1* in cell wall integrity [12]. Calcofluor white is a cell-wall stress agent that targets chitin and resistance indicates a specific deficiency in chitin deposition in the cell wall. Deletion of the main chitin synthase, Chs3, results in complete resistance to calcofluor white, whereas other cell wall mutants or overproduction of chitin results in sensitivity [13,34–36].

Both chitin and protein glycosylation are produced from the same precursor carbohydrate, UDP-GlcNAc, which is also the precursor for GPI anchors (Fig 1.2D). Chitin and GPI anchors predominantly function at the cell surface: GPI anchors are the major protein component of the cell wall, whereas chitin is a more minor, but still critical

structural component [14,18]. N-glycosylation functions on the cell surface as well, but is also essential for proper protein folding and trafficking [15]. Previous studies have shown that blocking GPI anchor formation increases chitin deposition in the cell wall [37]. UDP-GlcNAc synthesis is the rate-limiting step in the production of chitin, which is a polymer of UDP-GlcNAc, and GPI-anchor inhibition is thought to allow the accumulation of excess UDP-GlcNAc that is no longer converted into GPI anchors [17,37].

The tunicamycin sensitivity of the 2μ *ISR1* strain and the tunicamycin resistance observed in the *isr1*Δ strain might be due to misregulation of protein N-glycosylation. If *ISR1* overexpression specifically inhibited N-glycosylation, one would expect a larger pool of available UDP-GlcNAc for chitin synthesis, resulting in a compensatory increase in chitin production. However, we observed that 2μ *ISR1* caused resistance to calcofluor white, indicating a deficiency in chitin deposition. This is consistent with a defect in both protein glycosylation and chitin biosynthesis. This suggest that Isr1 acts upstream of N-glycosylation, reducing UDP-GlcNAc production.

Isr1 overexpression is synthetic lethal with enzymes in the hexosamine biosynthesis pathway

Most of the glucose imported into the cell is shunted into glycolysis after it is converted to fructose-6-phosphate, but approximately 6% enters the hexosamine biosynthesis pathway (HBP), where fructose-6-phosphate and glutamine are converted into UDP-GlcNAc though the sequential action of four enzymes: Gfa1, Gna1, Pcm1, and Qri1 (Fig 1.2D) [22]. This pathway is highly conserved from bacteria to humans [21].

Given that each of these enzymes are essential, we generated heterozygote deletions in genes encoding each of these enzymes and expressed GAL1-*ISR1* in these strains to test the genetic interactions of this pathway with *ISR1*. We found that GAL-2μ *ISR1* is synthetic lethal with all four enzymes in the pathway (Fig 1.2E). Notably, diploid wildtype cells are less sensitive to GAL-2μ *ISR1* as compared to haploid cells. Gln1 is not part of the HBP, but synthesizes glutamine, one of the precursors to the pathway [38], and also exhibits synthetic sickness in combination with GAL-2μ *ISR1*. These genetic interactions suggest that *ISR1* overexpression inhibits the HBP.

Isr1 lethality is rescued by exogenous glucosamine, but not other precursors to UDP-GlcNAc synthesis

The first enzyme of this pathway, Gfa1, converts fructose-6-phosphate and glutamine to glucosamine-6-phosphate (Fig 1.3A) [39]. This is the rate-limiting step of the pathway and Gfa1 activity is proportional to chitin synthesis [17]. *GFA1* essentiality can be by-passed by exogenous glucosamine, which can be phosphorylated by hexokinases. Thus, *gfa1*Δ strains are glucosamine auxotrophs. Addition of exogenous glucosamine drives flux through the HBP and increases UDP-GlcNAc production [39,40]. We tested if the lethality associated with GAL-2μ *ISR1* overexpression can be rescued by addition of exogenous glucosamine and found that in the presence of 5mM glucosamine, GAL-2μ *ISR1* no longer inhibited growth (Fig 1.3B). Some cell wall mutants have growth phenotypes that can be rescued by both exogenous glucosamine and by addition of sorbitol to the media [40]. As sorbitol is an osmotic stabilizer, this implies that the slow growth phenotype of such mutants is caused by cell lysis due to a

weakened cell wall. To determine if a similar general cell wall defect is responsible for the lethality associated with GAL-2μ *ISR1*, we tested growth of this strain in the presence of 10% sorbitol and found that sorbitol was not capable of rescuing growth (Fig 1.S1). This suggests that the lethality of GAL-2μ *ISR1* is due to a growth arrest caused by a deficiency of UDP-GlcNAc production and not cell lysis caused by a weakened cell wall.

As expected, addition of glucosamine also restored sensitivity of the 2μ *ISR1* overexpression strain to calcofluor white by driving flux through the HBP and increasing the amount of UDP-GlcNAc (Fig 1.3C). By contrast, glucosamine did not restore sensitivity to *chs3*Δ (Fig 1.3C), as an increase in UDP-GlcNAc cannot restore chitin synthesis in the absence of the chitin synthase itself. Thus, the resistance to calcofluor white observed upon 2μ overexpression of *ISR1* is unlikely to be due to a general trafficking defect that mislocalizes Chs3. This is in agreement with the lack of sensitivity observed upon exposure to DTT. Similarly, exogenous glucosamine restored growth to the 2μ *ISR1* strain in the presence of tunicamycin (Fig 1.3C). The ability of glucosamine to rescue *ISR1* overexpression phenotypes implies that Isr1 acts at or before the first step of the HBP. To determine if a deficiency in one of the precursors to the HBP is responsible for the *ISR1* overexpression phenotypes, we tested if fructose and glutamine, the reactants in the production of glucosamine-6-phosphate (Fig 1.3A), could rescue the *ISR1* overexpression phenotypes. We also tested alternative or non-fermentable carbon sources, which by-pass glycolysis entirely, and found that neither the precursors to the HBP nor non-fermentable carbon sources were capable of rescuing *ISR1* overexpression phenotypes (Figs 3C and 3D, Fig 1.S1). The ability of

glucosamine, but not precursors to the HBP, to completely rescue *ISR1* overexpression phenotypes indicates that Isr1 likely inhibits the first step of the HBP.

Isr1 is a negative regulator of GFA1

Our observation that exogenous glucosamine rescues the lethality associated with GAL-2μ *ISR1* overexpression suggests that Isr1 might inhibit flux through the HBP. If this is the case, overexpression of *GFA1* should rescue this lethality as well. To explore this possibility, we co-overexpressed *GFA1* on the same plasmid as *GAL1-ISR1* and as expected, *GFA1* overexpression also rescued the lethality associated with GAL-2μ *ISR1* overexpression (Fig 1.4A). To determine if this was unique to *GFA1,* we co-overexpressed another enzyme downstream in this pathway, Qri1, with *GAL1-ISR1*. *QRI1* only mildly increased growth on galactose, suggesting that Isr1 acts at the level of Gfa1 within the HBP (Fig 1.4A).

In other organisms, including *C. albicans*, drosophila, and humans, phosphorylation by multiple kinases, including AMPK and PKA, has been shown to both positively and negatively regulate Gfa1 activity [23–26,41,42]. Overexpression of *ISR1* did not alter Gfa1 protein levels (Fig 1.S2), suggesting that it might act by inhibiting Gfa1 function. However, the *GFA1-TAP* allele was unable to support viability and therefore it remains possible that the epitope tagged *GFA1* allele is stabilized or cannot be targeted by Isr1.

A previous mass spectrometry study of kinase interactors identified Gfa1 as a physical interactor with Isr1 in three separate immunoprecipitation experiments [43]. Given this, we sought to determine if Gfa1 is phosphorylated in an Isr1-dependent

manner. We conducted phosphoproteomics in *isr1*Δ cells expressing either an empty vector or GAL-2μ *ISR1* and detected over 8,779

distinct phosphorylated peptides on 1,860 proteins. In this experiment, we detected 4 sites of phosphorylation on Gfa1: S199, S253, S332, and T334. Of these sites, the doubly phosphorylated peptide containing S332 and T334 was 12.9-fold up-regulated in *ISR1*-expressing cells (Fig 1.4B). Additionally, a singly phosphorylated S332 peptide was also observed only in the *ISR1*-expressing cells. Targeted data extraction for this peptide revealed its phosphorylation level was 179-fold higher in *ISR1*-expressing cells (Fig 1.4C). To examine the importance of these phosphorylations, we mutated S332, T334, and S336 to alanine. S336 was included because it was adjacent to the other two sites and was seen to be phosphorylated in a previous whole-phosphoproteome screen [44]. Mutation of S332, T334, and S336 to alanine at the endogenous locus (referred to as *GFA1-3A*) rescued the lethality associated with GAL-2μ *ISR1* overexpression (Fig 1.4D). This suggests that Isr1 inhibits Gfa1 by promoting its phosphorylation.

Notably, the *GFA1-3A* mutant was slightly hypomorphic. While the *GFA1-3A* strain had no growth defect under normal conditions, it was sensitive to tunicamycin and resistant to calcofluor white (Fig 1.4E, S2C). This sensitivity was recessive, as expected for a hypomorph, and was epistatic to 2μ *ISR1* (Fig 1.4D, Fig 1.S2). By contrast, the *GFA1*-3A mutant was also dominant in its ability to rescue GAL-2μ *ISR1* -induced lethality: the *GFA1/GFA1-3A* heterozygous diploid was resistant to GAL-2μ *ISR1* (Fig 1.4F). Our finding that the resistance conferred by *GFA1-3A* is dominant is consistent with the hypothesis that *GFA1-3A* rescues *ISR1* overexpression because it is refractory to inhibition by Isr1. These data suggest Isr1 is a negative regulator of Gfa1.

It should be noted that, while the *GFA1* phosphomutant rescued GAL-2μ *ISR1* -induced lethality, *GFA1-3A* cells overexpressing *ISR1* still grew more slowly than *GFA1-3A* cells overexpressing *isr1-D280A*. Therefore, while our data support a model where Isr1 inhibits the HBP by promoting the phosphorylation of Gfa1, Isr1 may have additional substrates, additional sites on Gfa1, or both.

Isr1 is an unstable cell-cycle regulated protein targeted by Pho85 and Cdc4

Given that even mild overexpression of Isr1 inhibits the essential function of Gfa1, we next sought to understand how Isr1 is regulated in the cell. The cellular need for UDP-GlcNAc varies throughout the cell cycle and we therefore tested if Isr1 is a cell cycle regulated protein. Analysis of Isr1 protein levels after arresting cells in each phase of the cell cycle showed that Isr1 protein levels are largely confined to the G1/S transition and are drastically reduced in G1 and M phases (Fig 1.5A). This matches known transcriptional data for *ISR1* [45]. Previous work from our lab suggested that Isr1 is a substrate of Cdc4 [46]. Cdc4 is an F box protein that functions as a substrate adaptor for the SCF ubiquitin ligase complex and targets many substrates for proteasome-mediate degradation in a cell-cycle dependent manner [47]. Consistent with this, a cycloheximide chase of Isr1-13xMyc in wildtype cells, as compared to temperature-sensitive mutants of *CDC4* and *CDC53*, showed that Isr1 is unstable, with a half-life of approximately 30 minutes, and is stabilized by inactivation of *CDC4* or *CDC53* (Fig 1.5B).

Cdc4 recognizes and binds a phosphodegron with the optimal sequence (S/T)-P-X_{2-4}–(S/T) in which both (S/T) are phosphorylated, often by CDK kinases [48–51]. Isr1

was previously identified as an in vitro substrate of Pho85 [52], a CDK-like kinase that can function with any of 10 different cyclins in response to changes in nutrient and cell-cycle conditions [53,54]. Isr1 was shown to be phosphorylated by Pho85 in complex with Pcl1, which functions in G1 progression [52,55]. We found that deletion of *PHO85* stabilized Isr1, suggesting that Pho85-phosphorylation of Isr1 enables Isr1 to be targeted by Cdc4 for degradation (Fig 1.5C). Deletion of *PCL1* also partially stabilized Isr1 (Fig 1.5D). Given this partial stabilization, it remains possible that other Pcls, in addition to Pcl1, can also function with Pho85 to target Isr1. Pho85 is inhibited by the CDK inhibitor Pho81 in low phosphate conditions [56]. Upon release into low phosphate media, Isr1 levels increased, as would be expected if Pho85 activity promotes its instability (Fig 1.5E). Pho85 activity has also been shown to regulate carbohydrate metabolism [53,57]. We therefore tested if Isr1 stability was altered by carbon source. We found that growth in glycerol, a non-fermentable carbon source, as well as glucose withdrawal, also partially stabilized Isr1, whereas growth in galactose did not (Fig 1.S3). This supports a model where Pho85-mediated degradation of Isr1 might allow Isr1 activity to be responsive to environmental conditions.

Stabilization of an endogenous Isr1 phosphodegron recapitulates Isr1 overexpression phenotypes

Examination of the Isr1 protein sequence revealed two putative Cdc4 phosphodegrons in the N-terminus of the protein, each comprising two CDK consensus phosphorylation sites separated by several amino acids (Fig 1.6A). We constructed an *ISR1* phosphodegron mutant *(ISR1-PD)* by mutating these four residues (T4, S8, T86,

S92) as well as two adjacent serine/threonine residues to alanine at the endogenous locus. The *ISR1-PD* mutant was completely stable (Fig 1.6B), strongly supporting a model where phosphorylation of Isr1 at these sites targets it for degradation by Cdc4.

We next tested if this regulation is functionally relevant by examining the calcofluor white sensitivity of the *ISR1-PD* mutant. We found that these mutations are sufficient to cause resistance to calcofluor white, consistent with there being higher levels of Isr1 activity in *ISR1-PD* mutants (Fig 1.6C). This same resistance was recapitulated on Congo Red, a cell-wall stress agent that also targets chitin (Fig 1.S4) [58]. Similarly, the *ISR1-PD* mutant was also highly sensitive to tunicamycin (Fig 1.6D). Taken together, these data show that the endogenous phosphodegron mutant of Isr1 recapitulates *ISR1* overexpression phenotypes, supporting a model where tight regulation of Isr1 is critical for controlling its function in the cell. Interestingly, deletion of the entire N-terminal 93 amino acids of Isr1, which includes both phosphodegrons, was also sensitive to tunicamycin (Fig 1.6D). This implies that this truncation mutant is active and the only function of the N-terminus of Isr1 is in mediating its instability. Our mass spectrometry data also identified an additional proline-directed phosphorylation site in Isr1, S47, that may also be targeted by Pho85 or could represent autophosphorylation.

To determine the physiological relevance of Isr1 regulation, we tested the genetic interactions of this Isr1 phosphodegron mutant with deletions of the enzymes of the HBP pathway. Because these genes are essential, we examined diploids that were heterozygous for each HBP gene, as well as the *ISR1-PD* mutant. We found that *ISR1/ISR1-PD* showed a level of sensitivity to tunicamycin similar to that seen for *GFA1/gfa1*Δ (Fig 1.6E). One interpretation of this is that one copy of the stabilized Isr1

phosphodegron mutant reduces Gfa1 activity by half. Notably, The *GFA1/gfa1*Δ strain grew more slowly on tunicamycin than deletions of the other three enzymes in the pathway, as would be expected given that Gfa1 is the rate-limiting step of the pathway. While *ISR1/ISR1-PD* and *GFA1/gfa1*Δ were virtually synthetic lethal in the presence of tunicamycin, this synthetic sickness was not observed when *ISR1-PD* was combined with other deletions in the pathway. The specificity of this synthetic interaction further supports a model where Isr1 activity negatively regulates Gfa1 function and emphasizes the large effect of an even minor increase in Isr1 stabilization on flux through the HBP.

Discussion

Throughout the cell cycle and in response to changing nutrient conditions, the cell must balance its utilization of glucose for energy needs and as a precursor to structural and signaling carbohydrates. Here, we uncover a function for a previously uncharacterized kinase, Isr1, as a negative regulator of the hexosamine biosynthesis pathway (HBP) that synthesizes UDP-GlcNAc from glucose.

Isr1 previously had no ascribed function and its designation as a kinase was predicted based on homology to Raf [6]. Only ~15% of yeast genes are phenotypic when overexpressed [59]. The lethality of overexpressing *ISR1,* combined with the limited phenotypes of its deletion, support a model where Isr1 is a negative regulator of an essential protein. Our data firmly establishes a role for Isr1 in inhibition of the HBP based on several lines of evidence. First, 2μ overexpression of Isr1 results in resistance to calcofluor white and sensitivity to tunicamycin, whereas *isr1*Δ is slightly sensitive to calcofluor white and resistant to tunicamycin. These opposing phenotypes are consistent with a deficiency in UDP-GlcNAc when Isr1 is overexpressed and an increase in UDP-GlcNAc when Isr1 is absent. Genes that function in protein trafficking or the downstream utilization of UDP-GlcNAc in protein glycosylation are expected to have a compensatory increase in chitin production and to have a sensitivity to other ER-stress agents [37]. This was not observed for *ISR1* overexpression, suggesting that it inhibits the HBP itself. Consistent with this, we found that *ISR1* overexpression is synthetic lethal with every enzyme in the HBP.

All phenotypes of Isr1 overexpression are rescued by either overexpressing *GFA1*, the enzyme of the first step of the HBP, or by bypassing *GFA1* function by the

addition of exogenous glucosamine. Addition of reactants upstream of Gfa1, such as fructose and glutamine, had no effect. This strongly suggested that Isr1 inhibits this first step in the HBP. Furthermore, we found that phosphorylation of a specific serine in Gfa1 is dependent on Isr1 activity and mutation of this phosphorylation site to alanine rendered cells insensitive to *ISR1* overexpression. Thus, Isr1 appears to act as a negative regulator of Gfa1. The *GFA1* phosphomutant is hypomorphic, yet epistatic to *ISR1* overexpression and dominant in its ability to rescue GAL-2μ *ISR1* lethality, strongly implying that Isr1 exerts its function in the cell by promoting Gfa1 phosphorylation.

Isr1 may phosphorylate Gfa1 directly, as suggested by the existing immunoprecipitation -mass spectrometry data, or it might act in a kinase cascade. However, our phosphoproteomics dataset did not reveal specific activation of other kinases that might act downstream of Isr1. Notably, deletion of the majority of the N-terminal domain of Isr1 rendered Isr1 more active, implying that this portion of the protein is not required for substrate specificity. Given that the remaining residues comprise little more than a kinase domain, it remains unclear how Isr1 targets its substrates.

Additional genetic evidence suggests an interaction between *ISR1* and *GFA1*: Isr1 was identified due to the fact that its overexpression resulted in heightened sensitivity to staurosporine, an inhibitor of Pkc1 and *ISR1* deletion is synthetic lethal with a temperature sensitive allele of *PKC1* [6]. Pkc1 is known to positively regulate *GFA1* transcription through Rlm1 activation [27,60]. Therefore, this synthetic lethality is consistent with a role for Isr1 as a negative regulator of Gfa1. Similarly, *ISR1* has been

reported in multiple studies to have strong negative genetic interaction with *PRR1* [3,61,62], a kinase that is a physical interactor with Gfa1 [43]. These data would be consistent with Prr1 and Isr1 independently regulating Gfa1. Notably, *prr1*Δ does not rescue GAL-2μ *ISR1* lethality (Fig 1.S5).

The human homologue of Gfa1*,* Gfat1, has been previously shown to be negatively regulated by phosphorylation via AMPK and PKA [23,24,41]. Thus, inhibition of Gfa1 via phosphorylation may be a convergent or conserved mechanism of regulating hexosamine biosynthesis in response to changes in nutrients. The closest homologue of Isr1 in *S. pombe* is Byr2, which is a homologue of mammalian Raf and directly downstream of Ras [9]. While Isr1 is not thought to interact with Ras in *S. cerevisiae*, Ras2 has been shown to function downstream of the hexosamine biosynthesis pathway as a negative regulator of GPI anchor formation [37]. Ras2 inhibition of GPI anchor formation has been posited to allow remodeling of cell wall architecture in response to environmental stimuli by decreasing GPI-anchored proteins at the cell wall and, as a result of the increase in available UDP-GlcNAc, increasing chitin biosynthesis [37]. Thus, while Isr1 has diverged from the RAS/cAMP signaling pathway, it appears that both Isr1 and RAS work to integrate environmental signals to regulate the remodeling of the cell wall and glycoprotein biosynthesis.

The cellular requirement for UDP-GlcNAc changes throughout the cell cycle. While protein glycosylation occurs continuously as a cell grows, chitin synthesis predominates in G1 at the time of bud emergence [16]. Indeed, Gfa1 expression increases during G1 or in response to pheromone or cell wall stress [27,37,45]. Thus, dynamic control of Gfa1 is required to properly shunt glucose into or away from the

hexosamine biosynthesis pathway as needed. Notably, Isr1 protein levels peak at the G1/S transition, just after the period of time during the cell cycle at which higher levels of chitin synthesis are required. Given that Gfa1 activity is directly proportional to chitin synthesis [17], Isr1 might provide a mechanism of rapidly returning the cell to a normal level of chitin synthesis following bud emergence. Gfa1 is a highly abundant protein, whereas Isr1 is expressed at very low levels. We speculate that tight regulation of Isr1 protein levels via Pho85 and Cdc4 might allow for rapid dynamic changes in Gfa1 activity and could provide the cell with a less energetically costly mechanism of regulating Gfa1 function than degrading Gfa1 itself. While more studies are required to determine the specific environmental inputs that modulate Isr1 instability and the mechanism by which Isr1 inhibits Gfa1, this work firmly establish a cellular function for Isr1 as a key negative regulator of an essential, conserved pathway.

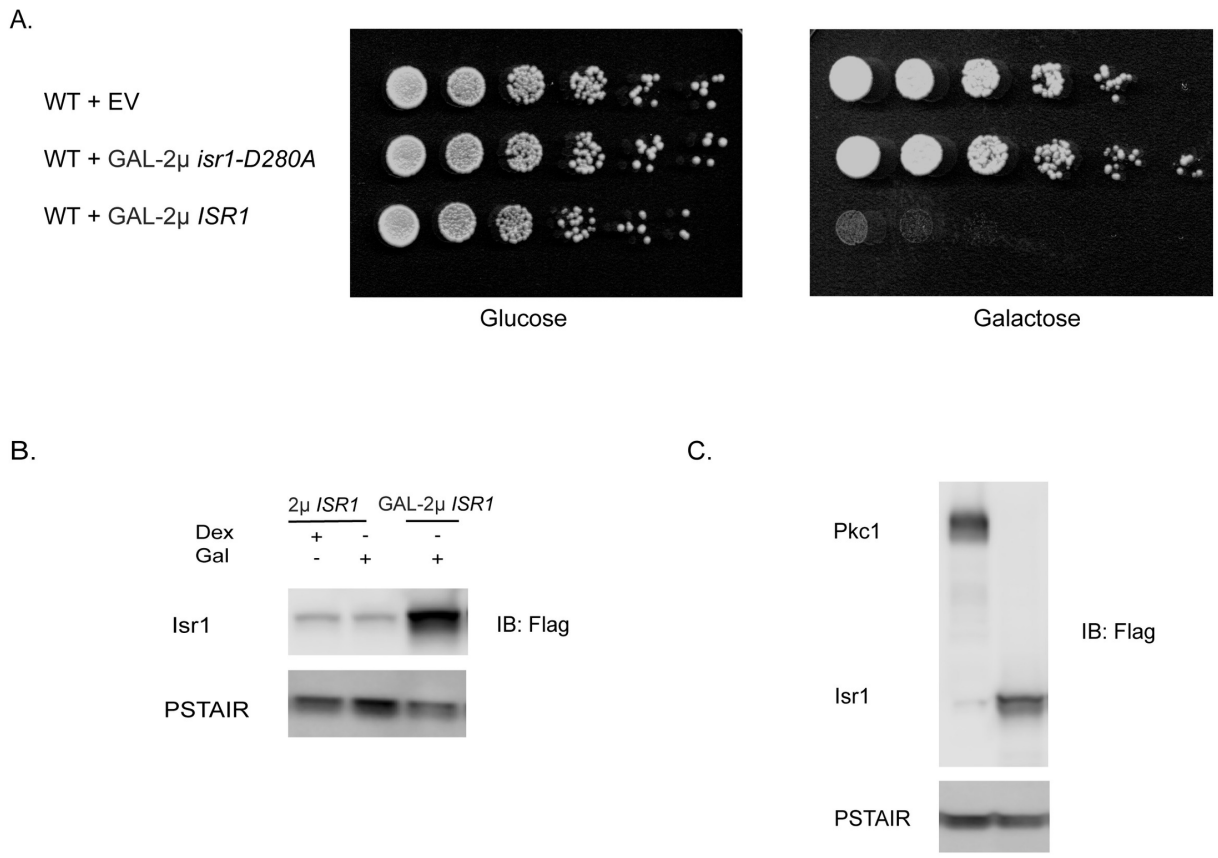

Fig 1.1. Overexpression of Isr1 is lethal.
(A) Wild type cells were transformed with an empty vector (EV) or 2μ plasmid expressing either a wildtype (GAL-2μ *ISR1*) or a kinase-dead allele of *ISR1* (GAL-2μ *isr1-D280A)* from the GAL1 promoter. Cells were serially diluted on YPD or YPGal plates. (B) Western blot showing relative expression level of Isr1-3xFlag expressed on a 2μ plasmid from either its endogenous promotor (2μ *ISR1*) or the *GAL1* promoter (GAL-2μ). Cells were inoculated into YM-1 with the indicated carbon source and grown for 4 hours under NAT selection. (C) Relative levels of Isr1-3xFlag expressed from the *GAL1* promoter compared to Pkc1-3xFlag tagged at the endogenous locus.

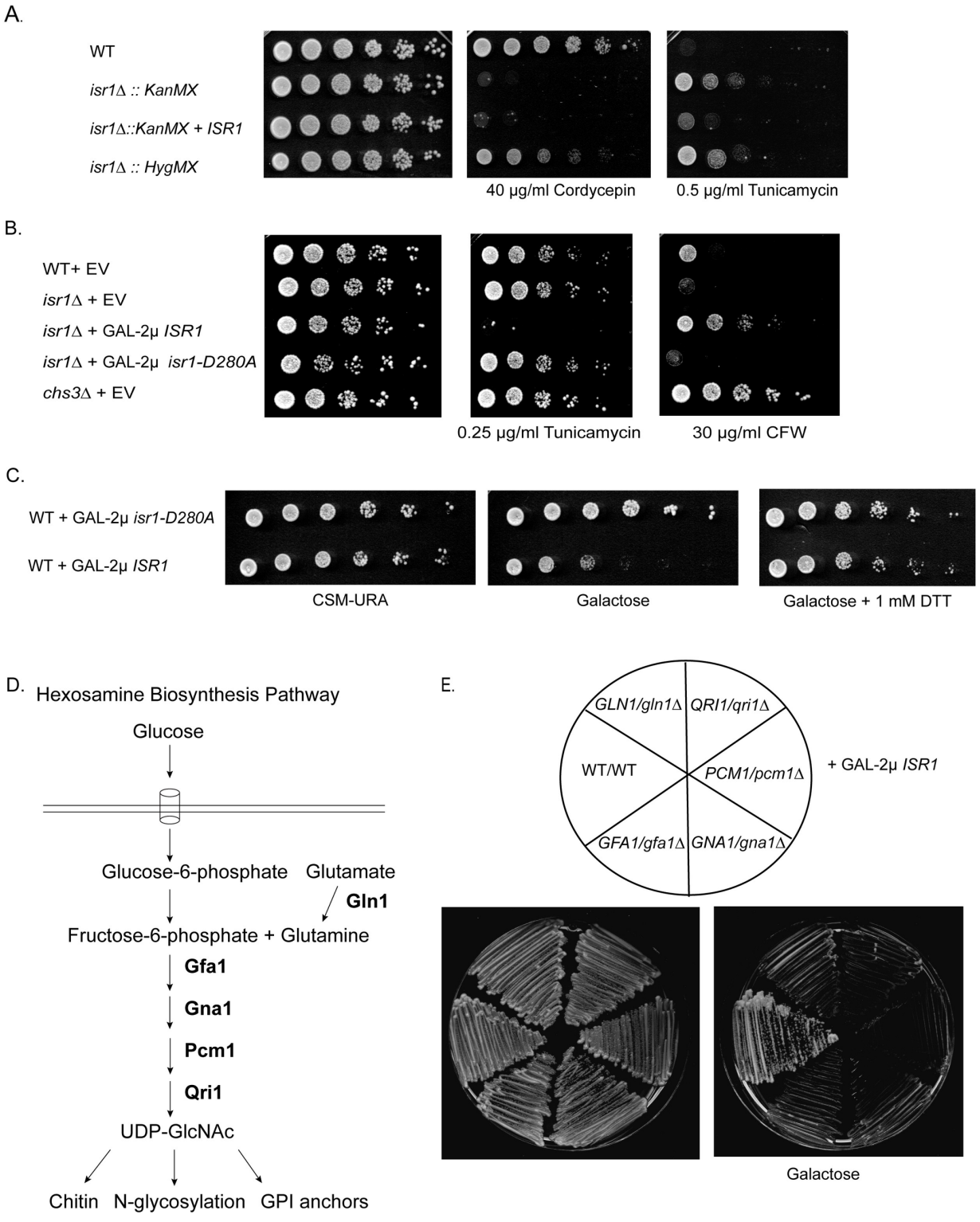

Fig 1.2. Altering *ISR1* dosage confers phenotypes associated with changes in flux through the hexosamine biosynthesis pathway.

(A) *isr1*Δ*::KanMX,* isolated from the *Mat a* deletion collection, exhibits a sensitivity to cordycepin that is not shared by *isr1*Δ*::HygMX* generated in this study. Both exhibit resistance to tunicamycin. Strains of the indicated genotypes were grown on YPD alone or containing 40 µg/ml cordycepin or 0.5 µg/ml tunicamycin. (B) 2µ *ISR1* causes sensitivity to tunicamycin and resistance to calcofluor white (CFW). Strains of the indicated genotypes were transformed with EV, or a 2µ plasmid expressing either a wildtype (2µ *ISR1*) or a kinase-dead allele of *ISR1* (2µ *isr1-D280A)* from the *ISR1* promoter. Strains were spotted on CSM in the presence or absence of 0.25 µg/ml tunicamycin or 30 µg/ml CFW. (C) Overexpression of Isr1 does not cause sensitivity to DTT. Wildtype cells were transformed with GAL-2µ *ISR1* or GAL-2µ *isr1-D280A* and spotted as in B on CSM-URA plates containing glucose, galactose or galactose + 1 mM DTT. (D) The hexosamine biosynthesis pathway converts fructose-6-phosphate and glutamine into UDP-GlcNAC, the precursor to N-glycosylation, GPI-anchors, and chitin. Gln1 acts upstream of the HBP and is required for glutamine synthesis. (E) GAL-2µ *ISR1* is synthetic lethal with all the enzymes in the HBP. Diploid heterozygous deletions of the enzymes in the HBP were generated and transformed with GAL-2µ *ISR1* and struck on YPD or YPGal plates. Note that wildtype diploids are less sensitive than haploid strains to Isr1 overexpression.

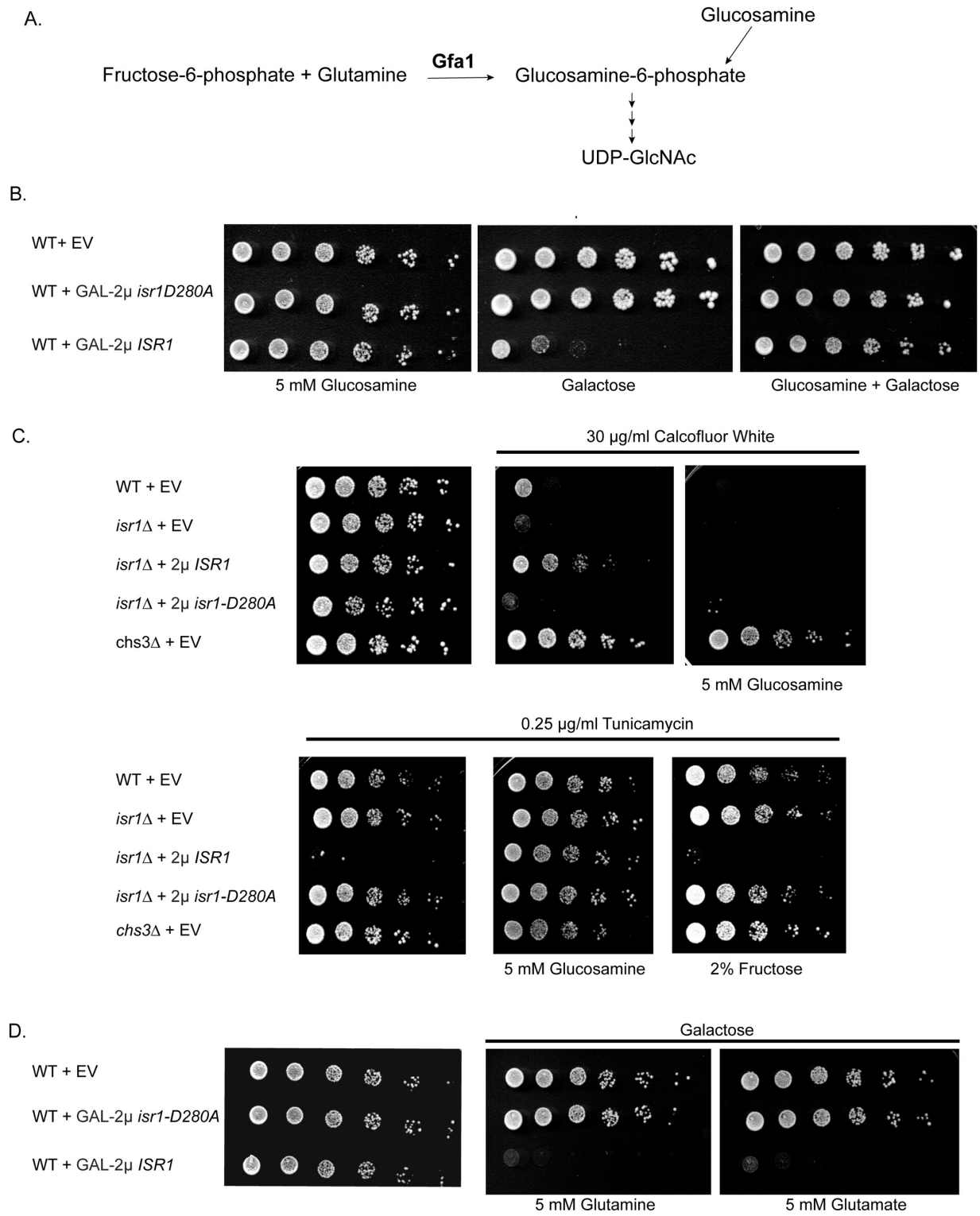

Fig 1.3: Exogenous glucosamine specifically rescues Isr1 overexpression phenotypes.

(A) Gfa1, the first and rate limiting enzyme in the HBP, converts fructose-6-phosphate and glutamine into glucosamine-6-phosphate. *GFA1* essentiality can be bypassed by

addition of exogenous glucosamine. (B) Exogenous glucosamine rescues GAL-2μ *ISR1* lethality. Wildtype cells were transformed with GAL-2μ *ISR1* or GAL-2μ *isr1-D280A* and spotted onto CSM + 5mM glucosamine, CSM galactose, or CSM galactose + 5mM glucosamine. (C) Exogenous glucosamine, but not fructose, restores resistance to tunicamycin and sensitivity to CFW. Strains of the indicated genotypes were transformed EV, 2μ ISR1, or 2μ *isr1-D280A*. Strains were spotted on CSM alone or containing 0.25 μg/ml tunicamycin, 30 μg/ml CFW, 5 mM glucosamine, or 2% fructose as indicated. (D) Lethality of GAL-2μ *ISR1* is not rescued by precursors to the HBP. Experiment was performed as in B and strains were spotted on CSM alone or CSM + galactose containing 5 mM glutamine or glutamate (MSG).

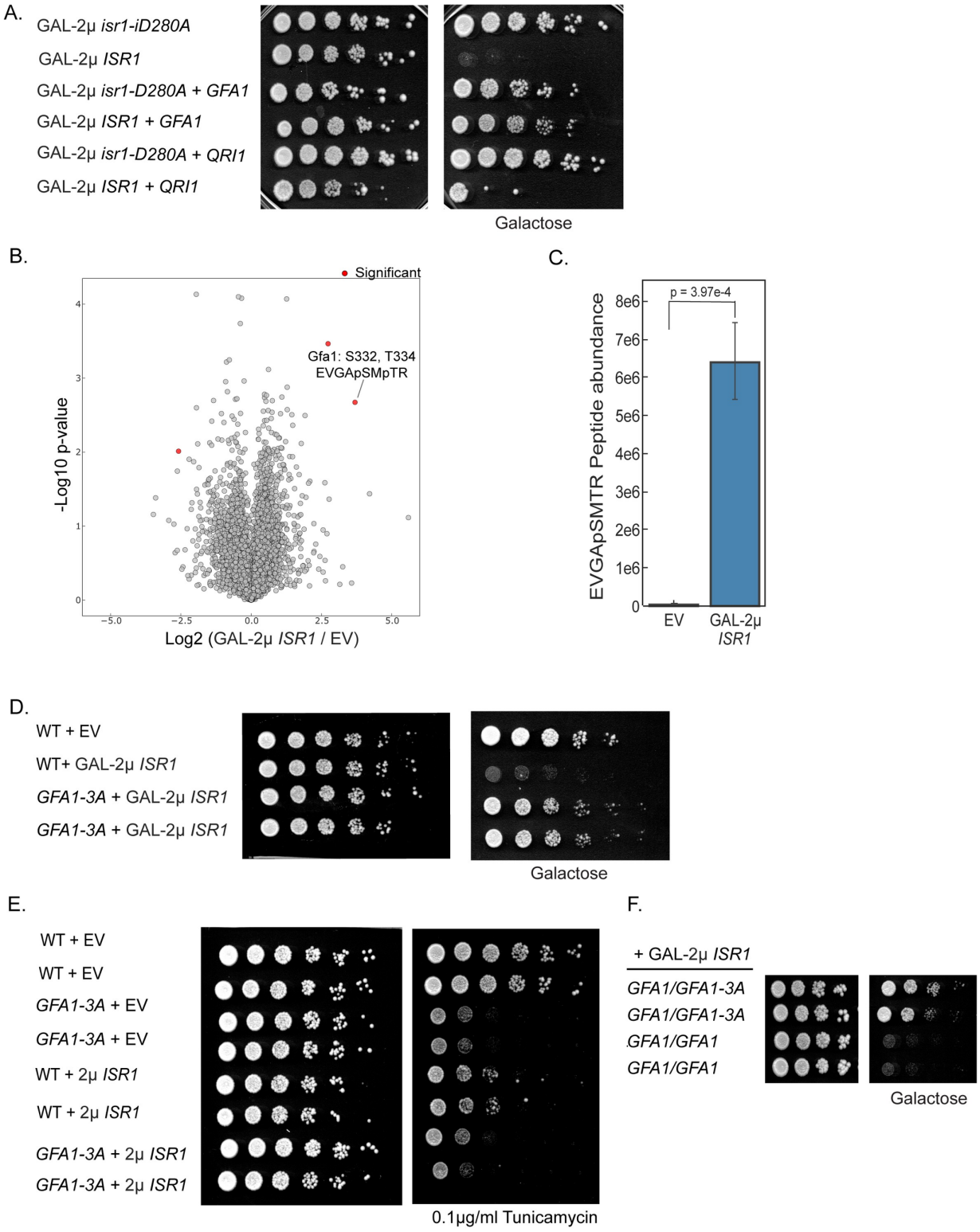

Fig 1.4. Gfa1 is phosphorylated in an Isr1-dependent manner and a *GFA1* phosphomutant rescues Isr1 lethality.

(A) *GFA1* overexpression rescues the lethality of GAL-2μ *ISR1*. Wildtype cells were transformed with a 2μ plasmid expressing either *ISR1* or *isr1-D280A* from the GAL1

promoter and either *GFA1* or *QRI1* from their endogenous promoters. Cells were serial diluted onto YPD or YPGal. (B) The Gfa1 S332 S334 phosphopeptide is enriched in cells expressing GAL-2μ *ISR1.* Volcano plot of phosphopeptides detected in *isr1*Δ cells expressing EV or GAL-2μ *ISR1*. Peptides with a $p < 0.01$ and having a fold change +/- 4-fold different between are considered significant. (C) Gfa1 S332 is phosphorylated in an Isr1-dependent manner. Targeted data extraction for Gfa1 S332 phosphorylation sites, which was only detected in the Gal-2u *ISR1* conditions. P-value is the result of a two-sided unpaired t-test. (D) Mutation of *GFA1* phosphorylation sites at the endogenous locus ameliorates the lethality of GAL-2μ *ISR1*. Wildtype cells or a *GFA1* phosphomutant (S332A,T334A, S336A) were transformed with EV or GAL-2μ *ISR1* and spotted as in A. (E) The *GFA1-3A* allele is hypomorphic. Cells of the indicated genotypes were transformed with EV or 2μ *ISR1* and serial diluted on YPD in the presence or absence of 0.1 μg/ml tunicamycin. (F) Experiment was performed as in D with diploid cells of the indicated genotypes.

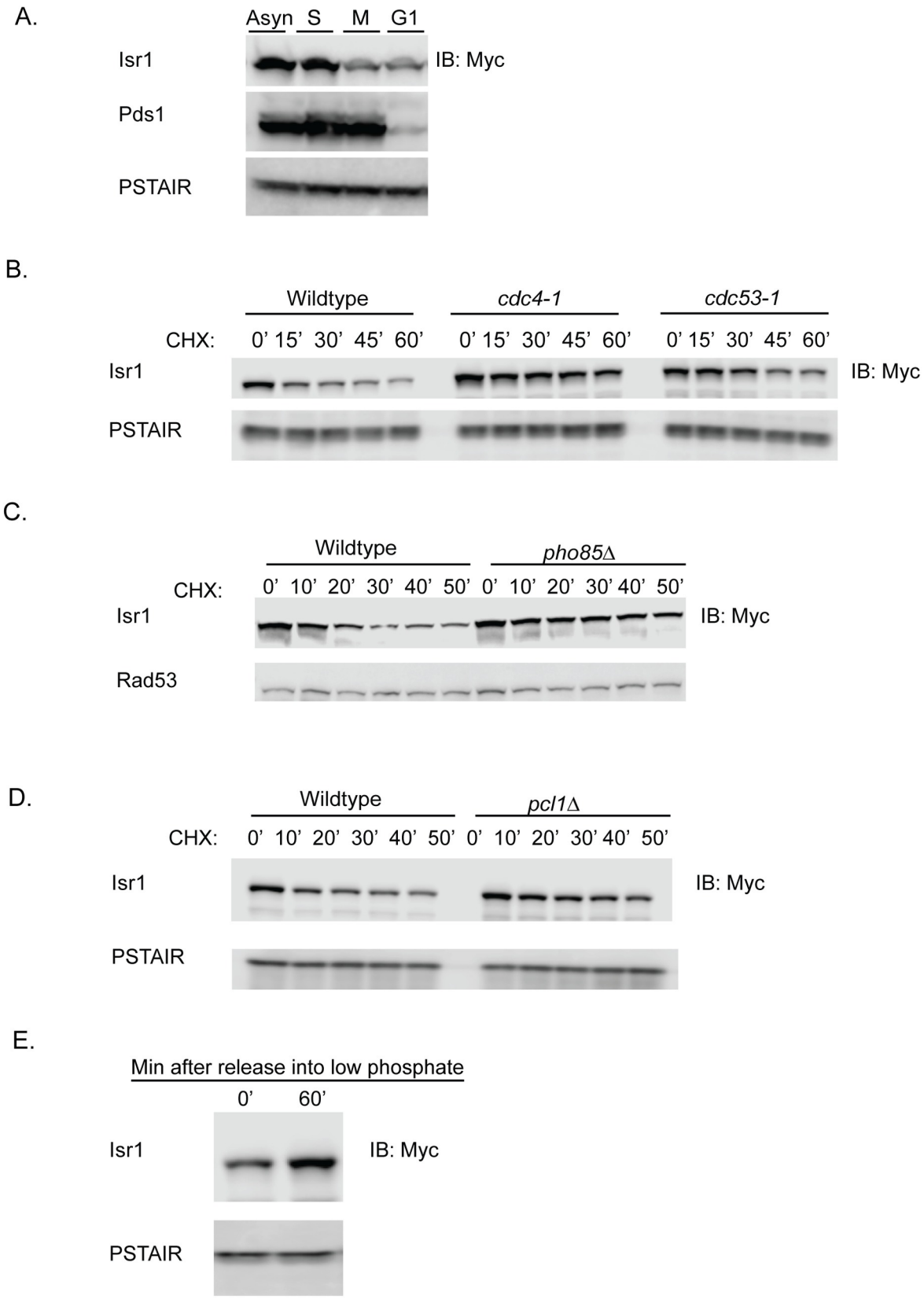

Fig 1.5. Isr1 is an unstable protein targeted by Pho85 and Cdc4.

(A) Isr1 is cell cycle regulated. Western blot showing levels of Isr1-13xmyc in cells growing asynchronously or arrested in G1, S, or M phase with alpha factor, Hydroxyurea (HU) or nocodazole, respectively. PSTAIR and Pds1 are shown as loading and cell cycle arrest controls, respectively. (B) Isr1 is targeted for degradation by Cdc4. Cycloheximide-chase assay of Isr1-13xmyc in wildtype, *cdc4-1,* or *cdc53-1* strains. Cells were shifted to the non-permissive temperature for 30 minutes before addition of cycloheximide for the indicated number of minutes. Levels of Isr1-13xMyc and PSTAIR (loading control) are shown. (C) Degradation of Isr1 is dependent on Pho85. Experiment was performed as in B at 30°C in *PHO85* or *pho85*Δ cells. Rad53 is shown as a loading control (D) Isr1 is stabilized by deletion of *PCL1*. Experiment as in B at 30°C in *PCL1* or *pcl1*Δ cells. (E) Western blot showing levels of Isr1-13xMyc and PSTAIR (loading control) after shifting cells to low phosphate media for 60 minutes.

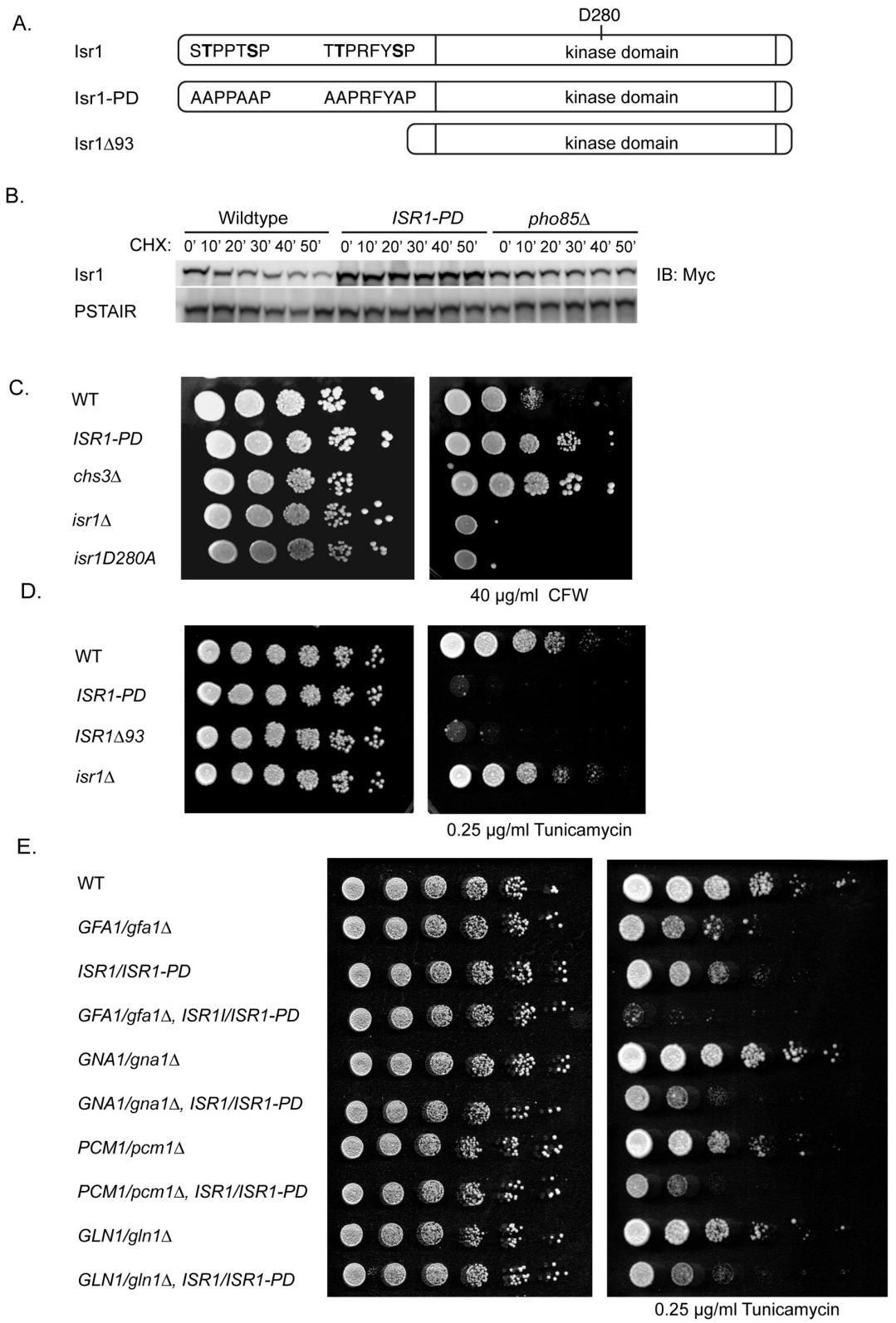

Fig 1.6. Stabilization of an endogenous Isr1 phosphodegron recapitulates overexpression phenotypes.

(A) Diagram of Pho85 and Cdc4 consensus sites in isr1 that comprise a phosphodegron. Six sites (T3, T4, S8, T85, T86, S92) are mutated to alanine in the *ISR1-PD* mutant. (B) An Isr1 phosphodegron mutant is stable. Cycloheximide-chase assay of Isr1-13xmyc in wildtype, *pho85*Δ, or cells expressing the phosphodegron mutant of *ISR1* from the endogenous locus (*ISR1-PD*). Cycloheximide was added for the indicated number of minutes. Levels of Isr1-13xMyc and PSTAIR (loading control) are shown. (C) An Isr1 phosphodegron mutant is resistant to calcofluor white (CFW). Strains of the indicated genotypes were diluted onto YPD with or without 40 μg/ml CFW. (D) An Isr1 phosphodegron mutant is sensitive to tunicamycin. Experiment was performed as in C, except strains were spotted on YPD with or without 0.25 μg/ml tunicamycin. (E) Diploid strains of the indicated genotypes were diluted onto YPD with or without 0.25 μg/ml tunicamycin.

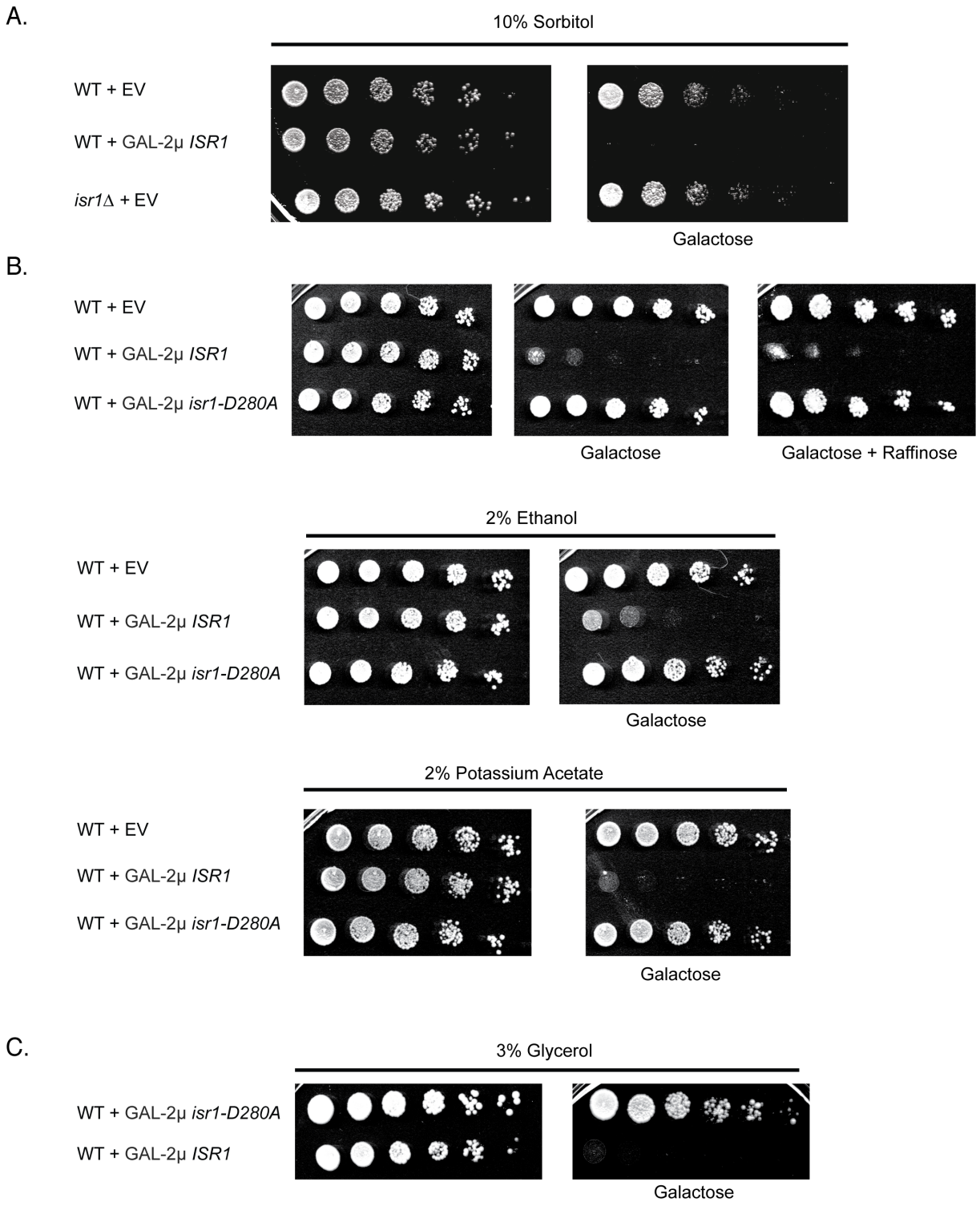

Fig 1.S1. Isr1 lethality is not rescued by osmotic stabilizers or other carbon sources.

(A) Lethality of GAL-2μ *ISR1* is not rescued by sorbitol. Cells of the indicated genotypes expressing EV or GAL- 2μ *ISR1* were diluted onto YPD or YPGal + 10% sorbitol. (B) Lethality from GAL- 2μ *ISR1* overexpression is not rescued by alternative carbon

sources. Wildtype cells were transformed with EV, GAL- 2μ *ISR1* or GAL- 2μ *isr1-D280A* and spotted onto CSM containing 2% glucose, galactose or the indicated carbon source. (C) Experiment performed as in B, but with 3% glycerol.

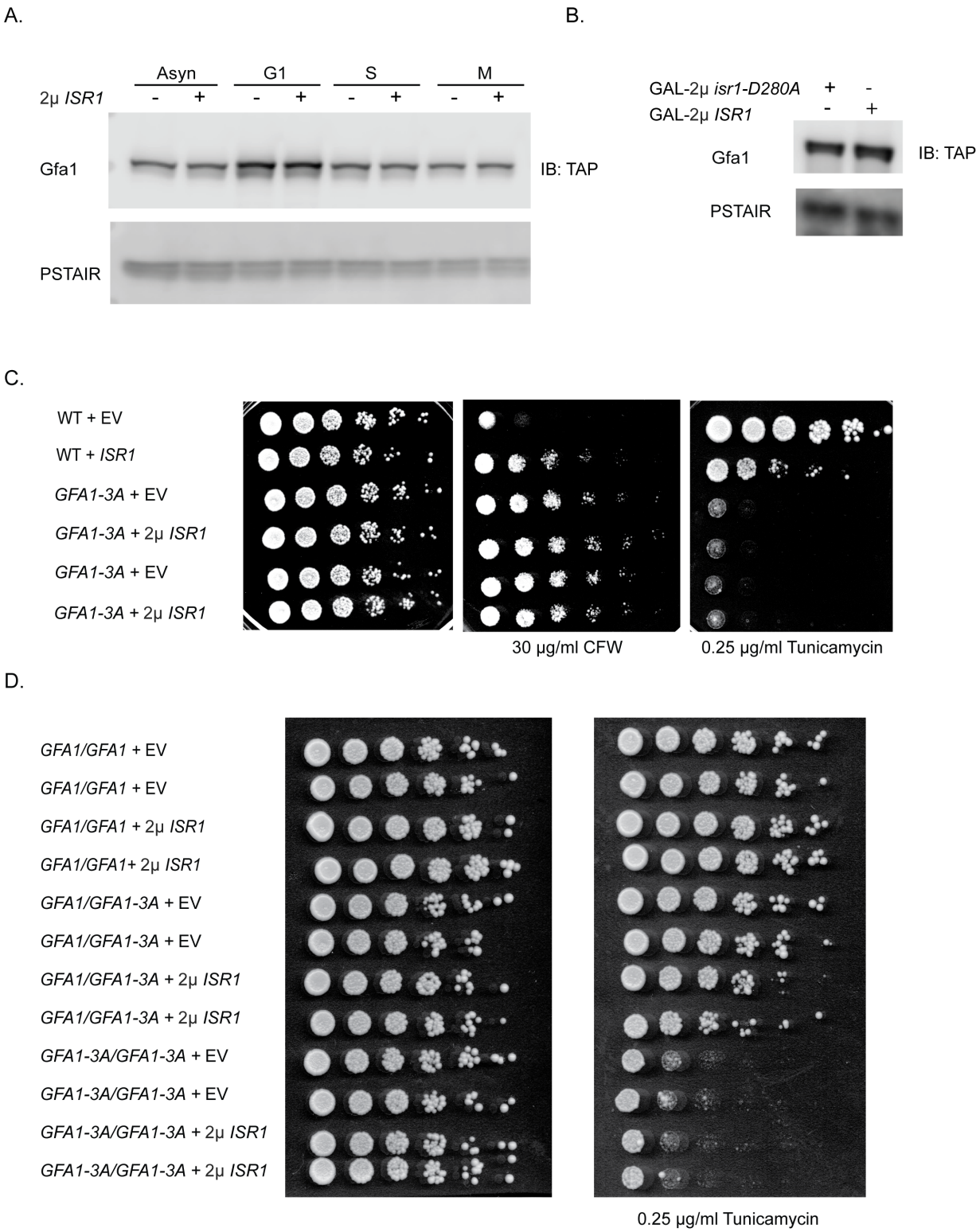

Fig 1.S2. Isr1 does not affect Gfa1 protein levels
(A). 2μ *ISR1* does not affect Gfa1 protein levels at any cell cycle stage. Cells were inoculated in CSM-URA and arrested in G1, S, and M phase with alpha factor, HU or nocodazole respectively. Note that Gfa1 was upregulated in response to alpha factor,

as expected. (B) GAL- 2μ *ISR1* does not alter Gfa1 protein levels. Cells were grown overnight in CSM-URA raffinose and inoculated in CSM-URA galactose for 4 hours. (C) Cells of the indicated genotypes were transformed with EV or 2μ *ISR1* and serial diluted on YPD with or without 30 μg/ml calcofluor white. (D) Diploids of the indicated genotypes were transformed with EV or 2μ *ISR1* and spotted on YPD with or without 0.25 μg/ml tunicamycin.

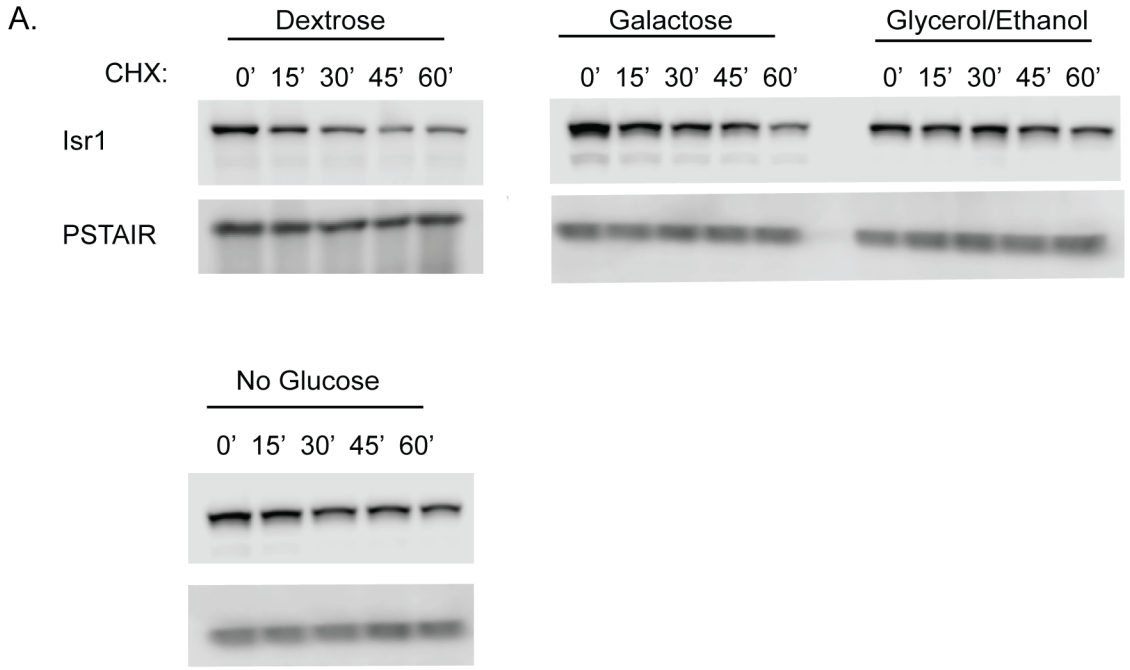

Fig 1.S3. Isr1 is partially stabilized in non-fermentable carbon sources
(A) Isr1 is partially stabilized by glycerol/ethanol, but not galactose. Cycloheximide-chase assay of Isr1-13xmyc grown in YM-1 containing 2% dextrose, 2% galactose or 2% glycerol/1% ethanol. Cells were grown overnight in the indicated carbon source, inoculated in fresh media, and cycloheximide was added at 0.5 OD/ml for the indicated number of minutes. For the no glucose condition, cells were grown in YM-1 with dextrose, washed twice in media without a carbon source, and suspended in media with no carbon source at the same time as adding cycloheximide.

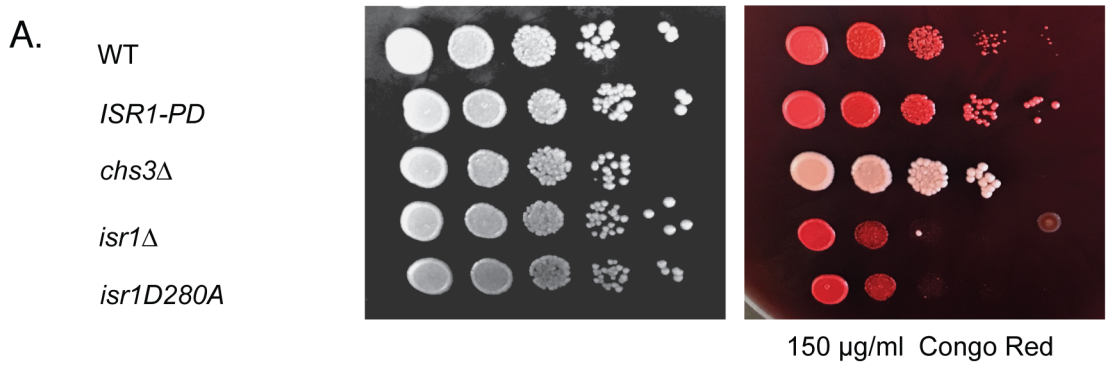

Fig 1.S4. Mutation of an Isr1 phosphodegron confers resistance to Congo Red
(A) An Isr1 phosphodegron mutant is resistant to Congo Red. Strains of the indicated genotypes were diluted onto YPD in the presence or absence of 150 µg/ml Congo Red.

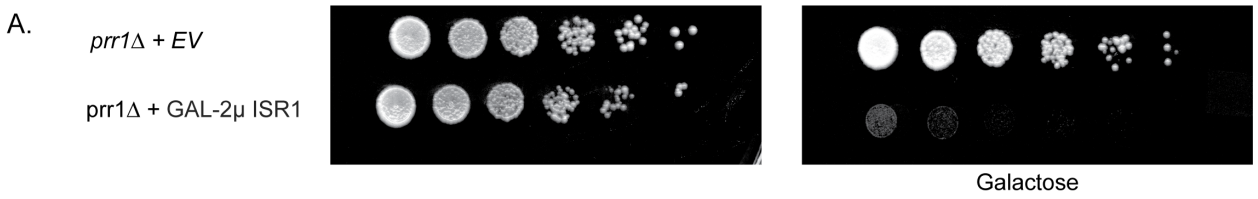

Fig 1.S5. *PRR1* is not downstream of ISR1
*(A) prr1*Δ cells expressing EV or Gal- 2μ *ISR1* were serial diluted onto YPD or YPGal.

GTGATGTATGGGTCTATCTTATTGTTTATTTTGACTAGCATTGAATAAACAAAAAGC

GCTGCTAATAGATTCTTGCCTTTATATAACGGGGATCTAACCTCATCAACAGCAAAA

ATCGTCTTAAAACACATCTCAAAGACTAGTTCTCAAACGTCACGCTATGAACgctgCA

CCTCCTgccgCACCCGTCACCAGGGTTTCTGATGGTTCCTTTCCATCCATAAGTAAC

AATAGTAAGGGTTTTGCTTATCGCCAACCGCAAAAACATAAAAGTAACTTCGCATAT

TCACATCTGGTATCTCCTGTAGAGGAGCCGACAGCTAAATTCAGTGAGGCATTCCA

GACAGATTATTCTAGTAAGGCGCCCGTTGCTACCTCGGAGGCGCACCTAAAGAAC

GATTTAGACGTATTGTTCgCTgCCCCCCGGTTTTACgCTCCGGAGAATTTGGCTTTA

ATGTTCCGTCTTTCTAATACAGTTTCTTCCCTAGAATTTCTGGATGAGTTTTTGATGG

GCATATTACTTGCTCCAGAGATGGATTTTTTGTCAAATCCAAGTTATTCTCTTCCGT

CTAACAAATTAGTGGGACAGGGAAGTTATTCATATGTGTACCCTATATCATCAAGTG

CTTCATCAAGATGTAACAACGATTCAGGGGTTGTTTTAAAGTTTGCCAAATCACAGC

ATAAAAGCAAGGTGATTTTACAGGAAGCTTTGACGCTAGCATATCTCCAGTACATG

AGTCCTTCAAC

Fig 1.S6. ISR1 Phosphodegron mutant sequence
Double-stranded DNA sequence used to generate ISR1 phosphodegron mutant. Blue sequence is the end of the Isr1 promoter. Lowercase red base pairs indicate mutated residues.

Table 1.S1. Strains used in this study

Strain Name	Genotype	Fig
BY4741	*MATa his3Δ1 leu2Δ0 met15Δ0 ura3Δ0*	
EBA142	*MATa his3Δ1 ura3Δ0 leu2Δ0 met15Δ0 isr1Δ::KanMX*	2A
EBA211	*MATa his3Δ1 ura3Δ0 leu2Δ0 met15Δ0 isr1Δ::HygMX*	2A, 3C, 3D, 4B, 4C, 6C, 6D, S4
EBA206	*MATa his3Δ1 ura3Δ0 leu2Δ0 met15Δ0 Pkc1-3xFlag::KanMX*	1C
EBA183	*MATa his3Δ1 ura3Δ0 leu2Δ0 met15Δ0 ISR1-13xmyc::NAT*	6C, 6D, S4
EBA185	*MATa his3Δ1 ura3Δ0 leu2Δ0 met15Δ0 ISR1-PD13xmyc::NAT*	6C, 6D, 6E, S4A
EBA176	*MATa his3Δ1 ura3Δ0 leu2Δ0 met15Δ0 isr1D280A::NAT*	6C, 6D, S4
EBA151	*MATα his3Δ1 ura3Δ0 leu2Δ0 lys2Δ0 chs3Δ::KanMX*	2B,6C, 6D, S4
EBA160	*MATa his3Δ1 ura3Δ0 leu2Δ0 met15Δ0 GFA1-TAP-His3MX*	S2
EBA329	*MATa his3Δ1 ura3Δ0 leu2Δ0 met15Δ0 GFA1-3A::HygMX*	4D, 4E, S2
EBA330	*MATa his3Δ1 ura3Δ0 leu2Δ0 met15Δ0 GFA1-3A::HygMX*	4D, 4E, S2
EBA326	*MATa/MATα his3Δ1/ his3Δ1 ura3Δ0/ ura3Δ0 leu2Δ0/ leu2Δ0 MET15/met15Δ0 LYS2/lys2Δ0 GFA1/GFA1-3A::HygMX*	4F, S2
EBA327	*MATa/MATα his3Δ1/ his3Δ1 ura3Δ0/ ura3Δ0 leu2Δ0/ leu2Δ0 MET15/met15Δ0 LYS2/lys2Δ0 GFA1/GFA1-3A::HygMX*	4F, S2
EBA114	*MATa/MATα his3Δ1/ his3Δ1 ura3Δ0/ ura3Δ0 leu2Δ0/ leu2Δ0 MET15/met15Δ0 LYS2/lys2Δ0*	2E, 4F, 6E, S2
EBA268	*MATa/MATα his3Δ1/ his3Δ1 ura3Δ0/ ura3Δ0 leu2Δ0/ leu2Δ0 MET15/met15Δ0 LYS2/lys2Δ0 ISR1/ISR1-PD::NAT*	6E
EBA273	*MATa/MATα his3Δ1/ his3Δ1 ura3Δ0/ ura3Δ0 leu2Δ0/ leu2Δ0 MET15/met15Δ0 LYS2/lys2Δ0 GFA1/gfa1Δ::KanMX*	2E, 6E, S2
EBA269	*MATa/MATα his3Δ1/ his3Δ1 ura3Δ0/ ura3Δ0 leu2Δ0/ leu2Δ0 MET15/met15Δ0 LYS2/lys2Δ0 GFA1/gfa1Δ::KanMX ISR1/ISR1-PD::NAT*	6E
EBA368	*MATa/MATα his3Δ1/ his3Δ1 ura3Δ0/*	S2

Strain Name	Genotype	Fig
	ura3Δ0 leu2Δ0/ leu2Δ0 MET15/met15Δ0 LYS2/lys2∆0 GFA1-3A/GFA1-3A::HygMX	
EBA369	*MATa/MATα his3Δ1/ his3Δ1 ura3Δ0/ ura3Δ0 leu2Δ0/ leu2Δ0 MET15/met15Δ0 LYS2/lys2∆0 GFA1-3A/GFA1-3A::HygMX*	S2
EBA315	*MATa/MATα his3Δ1/ his3Δ1 ura3Δ0/ ura3Δ0 leu2Δ0/ leu2Δ0 MET15/met15Δ0 LYS2/lys2∆0 GNA1/gna1∆::KANMX ISR1/ISR1-PD::NAT*	6E
EBA316	*MATa/MATα his3Δ1/ his3Δ1 ura3Δ0/ ura3Δ0 leu2Δ0/ leu2Δ0 MET15/met15Δ0 LYS2/lys2∆0 GNA1/gna1∆::∆::KANMX*	2E, 6E
EBA302	*MATa/MATα his3Δ1/ his3Δ1 ura3Δ0/ ura3Δ0 leu2Δ0/ leu2Δ0 MET15/met15Δ0 LYS2/lys2∆0 GLN1/gln1∆::KANMX ISR1/ISR1-PD::NAT*	6E
EBA319	*MATa/MATα his3Δ1/ his3Δ1 ura3Δ0/ ura3Δ0 leu2Δ0/ leu2Δ0 MET15/met15Δ0 LYS2/lys2∆0 PCM1/pcm1∆::KANMX*	2E, 6E
EBA328	*MATa/MATα his3Δ1/ his3Δ1 ura3Δ0/ ura3Δ0 leu2Δ0/ leu2Δ0 MET15/met15Δ0 LYS2/lys2∆0 PCM1/pcm1∆::KANMX ISR1/ISR1-PD::NAT*	6E
EBA304	*MATa/MATα his3Δ1/ his3Δ1 ura3Δ0/ ura3Δ0 leu2Δ0/ leu2Δ0 MET15/met15Δ0 LYS2/lys2∆0 QRi1/qri1∆::KANMX*	2E, 6E
EBA303	*MATa/MATα his3Δ1/ his3Δ1 ura3Δ0/ ura3Δ0 leu2Δ0/ leu2Δ0 MET15/met15Δ0 LYS2/lys2∆0 QRi1/qri1∆∆::KANMX ISR1/ISR1-PD::NAT*	6E
EBA135	*MATa his3Δ1 ura3Δ0 leu2Δ0 met15Δ0 lsr1-13xmyc::URA3*	5A-E, 6B, S3
EBA153	MATa his3Δ1 ura3Δ0 leu2Δ0 met15Δ0 pho85∆::KANMX lsr1-13xmyc::URA3	5C, 6B
EBA332	MATa his3Δ1 ura3Δ0 leu2Δ0 met15Δ0 cdc4-1::HYGMX lsr1-13xmyc::URA3	5B
EBA158	MATα his3Δ1 ura3Δ0 leu2Δ0 lys2∆0 cdc53-1 lsr1-13xmyc::URA3	5B
EBA331	MATa his3Δ1 ura3Δ0 leu2Δ0 met15Δ0 pcl1∆::KANMX lsr1-13xmyc::URA3	5C
EBA174	MATa his3Δ1 ura3Δ0 leu2Δ0 met15Δ0 3xHA-lsr1∆93::NATMX	6D
knockout collection	MATa his3Δ1 ura3Δ0 leu2Δ0 met15Δ0 YFGΔ::KANMX	

Table 1.S2. Plasmids used in this study

Plasmid Name	Description	Fig/Use
EBP294	Prs426 NAT (EV)	1A, 2B, 3B, 3C, 3D, 4D, 4E, S1, S2, S5
EBP187	2µ *ISR1*	1B, 2B, 3C, 4E, S2
EBP290	2µ *ISR1 isr1-D280A*	2B, 3C
EBP211	Gal- 2µ *ISR1*	1, 2C, 2E, 3B, 3D, 4A, 4B, 4C, 4D,4F, S1, S2, S5
EBP210	Gal- 2µ *isr1-D280A*	1A, 2C, 3B, 3D, 4A, S1, S2
EBP215	prs426NAT + *GAL1-ISR13xFlag*, *GFA1pr-GFA1*	4A
EBP216	pr*s426NAT* + *GAL1-isr1D280A-3xFlag, GFA1pr-GFA1*	4A
EBP211	prs426NAT + *GAL1-ISR1-3xFlag*, *QRI1pr-QRI1*	4A
EBP212	prs426NAT + *GAL1-isr1D280A-3xFlag*, *QRI1pr-QRI1*	4A
EBP168	prs402NAT + *ISR1pr-ISR1-13xMyc*	Construction of *ISR1* integration (wildtype)
EBP181	prs402NAT + *ISR1pr-ISR1PD-13xMyc*	Construction of *ISR1-PD* integration
EBP172	prs402NAT + *ISR1pr-isr1D280A*	Construction of *isr1-D280A* integration
EBP220	p3xFlagHYGMX + *GFA1*	Construction of *GFA1*

Plasmid Name	Description	Fig/Use
		integration (WT)
EBP223	p3xFlagHYGMX + *GFA1-S332AT334AS336A*	Construction of *GFA1-3A* integration
MS197	Prs306 + *ISR1-13xMyc*	Construction of *ISR1-13xmyc* tagged strains
PYMN-20	PYMN-20 (66)	Construction of *HA-ISR1Δ93*

Materials and Methods

Strains and Plasmids

Strains and plasmids used in this study are listed in Tables S2 and S3, respectively. All yeast strains in this study are in the S288C background. Unless otherwise noted, single gene deletions are from the *Mat a* deletion collection (Open Biosystems) and TAP-tagged strains were a gift from Erin O'Shea and Jonathan Weismann. Cloning of constructs and transformations were done using standard techniques. Diploid heterozygous deletions were made by transformation of a *KanMX* cassette with homology to the promoter and 3' UTR of the gene of interest into a wild type diploid or heterozygous *ISR1-PD* diploid strain. The *ISR1-PD* and *GFA1-3A* strains were constructed by gene replacement: point mutants were synthesized on a plasmid containing a nourseothricin (NAT) (ISR1) or *HygMX (GFA1)* selection marker (Table 1.S2, Fig 1.S6). A PCR fragment was generated with homology to the endogenous promoter at the 5' end and the MX cassette at the 3' end. This PCR fragment was transformed into the deletion strain to replace the gene deletion previously marked by *HygMX (ISR1*) or *KanMX (GFA1).* Integrations were screened by marker loss/gain and then verified by PCR. In the case of *GFA1*, *GFA1-3A* was first generated in a *GFA1/gfa1*Δ diploid and haploid mutants were isolated by tetrad analysis.

Yeast Cell Culture

Selective media lacking specific amino acids or nucleobases was made using Complete Supplement Mixture (CSM) from Sunrise Sciences, supplemented with yeast nitrogen base and 2% dextrose. Unless otherwise noted, cells were cultured at 30°C on YM-1

media supplemented with 2% dextrose or CSM-URA to maintain plasmid selection. 100 µg/ml NAT was added to maintain plasmids when strains were grown in YM-1. Expression from the *GAL1* promoter was induced with 2% (wt/vol) galactose for 4 hours. For experiments with temperature-sensitive strains, cells were maintained at 23 °C and shifted to 37°C for 30 minutes before initiating the experiment. Low phosphate media was made as with CSM, but using YNB lacking amino acids and phosphate (Formedium CYN0803) and supplemented with 0.55g KCl/liter. To measure Isr1 protein levels in low phosphate, cells were washed several times in low-phosphate media and resuspended in low-phosphate media for 60 minutes.

Western Blotting

From cultures in midlog phase, cell pellets of equivalent optical densities were collected, washed with 1 mL 4°C H_2O, and frozen on dry ice. Standard TCA precipitations were preformed to extract proteins. Samples were resuspended in SDS-PAGE sample buffer, boiled for 5 min, and cell lysates were analyzed by SDS-PAGE using 4–20% gradient Tis-HCl gels (BioRad, #3450034). Proteins were transferred onto 0.2-µm nitrocellulose membrane. Western blots were performed with low-salt PBS with Tween-20 (PBS-T) (15 mM NaCl, 1.3 mM NaH_2PO_4, 5.4 mM Na_2HPO_4, 0.05% Tween-20). Primary antibody incubations were performed in 5% (wt/vol) nonfat dry milk and low-salt PBS-T. Antibodies were used as follows: α-Rad53 (Abcam ab104232); α-Flag (Sigma-Aldrich, F3165); α-Myc (BioLegend, #626802), α-PSTAIR (Sigma-Aldrich P7962), α-Pds1 (generous gifts from Adam Rudner), α-TAP (Thermo-Scientific CAB1001). Western blots were visualized by LiCor Odyssey Imaging System.

Cell Cycle Arrest

Cells were grown overnight in YM-1 and inoculated to OD600 = 0.2 and grown at 30°C for 45 minutes. For arrest in G1, 15 µg/mL alpha factor was added. After 90 minutes, an additional 10 µg/mL alpha factor was added. Cells were harvested after 2.5 hours. For arrest in S and M phase respectively, 200 mM HU or 15 µg /ml nocadozole was added and cells were harvested after 2 hours. Arrest was confirmed by microscopic analysis and equivalent ODs were processed for western blots as described above.

Cycloheximide-Chase Assays

Cells were grown as for western blotting to midlog phase. Cycloheximide was added to cultures for a final concentration of 50 µg/mL after collection at the t = 0 time point. Equivalent ODs were collected for each time point and were processed for western blots as described above. For *cdc53-1* and *cdc4-1* experiments, cells (including wild type control) were shifted to 37 °C for 30 minutes before addition of cycloheximide. For alternative carbon sources, cells were grown overnight in YM-1 supplemented with 2% dextrose, 2% galactose or 2% glycerol/1% ethanol, inoculated at 0.2 OD, and grown to mid-log phase before addition of cycloheximide.

Mass Spectrometry

Cell lysis and sample preparation. Cells were grown overnight in YM-1 supplemented with 2% raffinose and 100 µg/ml NAT and then inoculated at 0.3 OD. After 1 hour, 40% galactose was added to a final concentration of 2% galactose and cells were grown for

an additional 3 hours to OD ~0.8. 40 OD of cells were washed 2x with water and flash frozen in liquid nitrogen. Cells pellets were combined and lysed in a denaturing urea buffer (8 M urea, 0.1 M ammonium bicarbonate, pH 8, 150 mM NaCl, 1 Roche mini protease inhibitor tablet without EDTA/10 ml, ½ Roche phosSTOP tablet/10 ml) using 14 × 1.5 min bursts on a BioSpec mini bead-beater at room temperature. 2 ml screw-cap tubes used for lysis were pierced with an 18-gauge needle and spun in a swinging bucket centrifuge for 30 s at 1000 × *g* to collect extract. Extract was rotated end-over-end for 30 min at room temperature before clarification via centrifugation at 17,000 × *g* for 7 min followed by a second centrifugation at 17,000 × *g* for 2 min, both at room temperature. Extracts were quantitated using a BCA protein quantification kit (Pierce). 1 M TCEP (Sigma C4706–2) was added to final concentration of 4 mM to 1 mg of protein and incubated for 30 min at room temperature. 0.5 M iodoacetamide (Sigma L1149–5G, prepared fresh in water) was added to a final concentration of 10 mM and incubated in the dark for 30 min. To quench excess iodoacetamide, 0.5 M DTT was added to a final concentration of 10 mM for another 30 min in the dark. Samples were diluted ~fourfold (to less than 2 M urea) with 0.1 M Tris, pH 8, and Lys-C/trypsin (Promega, Madison, WI, V5071, dissolved in 50 mM acetic acid) was added at a ratio of 200 ug trypsin to 1 mg total protein. Samples (~1 ml total volume of diluted sample) were incubated for 20 hours at room temperature with rotation. After digestion, TFA was added to a final concentration of 0.3–0.1% TFA, with pH of final solution ~2.

Phosphopeptide enrichment by immobilized metal affinity chromatography. Iron nitrilotriacetic acid (NTA) resin were prepared in-house by stripping metal ions from nickel nitrilotriacetic acid agarose resin (Qiagen) with 100 mM

ethylenediaminetetraacetic (EDTA) acid, pH 8.0 three times. Resin was washed twice with water and 100 mM iron(III) chloride was applied three times. The iron-NTA resin was washed twice with water and once with 0.5% formic acid. Iron-NTA beads were resuspended in water to create a 25% resin slurry. 60 µl of Fe-NTA resin slurry was transferred to individual Silica C18 MicroSpin columns (The Nest Group) pre-equilibrated with 100 µl of 80% ACN, 0.1% TFA on a vacuum manifold. Subsequent steps were performed with the Fe-NTA resin loaded on the Silica C18 columns. Peptide samples were mixed twice with the Fe-NTA resin and allowed to incubate for 2 minutes. The resin was rinsed four times with 200 µl of 80% ACN, 0.1% TFA. In order to equilibrate the chromatography columns, 200 µl of 0.5% formic acid was applied twice to the resin and columns. Peptides were eluted from the resin onto the C18 column by application of 200 µl of 500 mM potassium phosphate, pH 7.0. Peptides were washed twice with 200 µl of 0.5% formic acid. The C18 columns were removed from the vacuum manifold and eluted twice by centrifugation at 1000*g* with 60 µl of 50% ACN, 0.25% TFA. Peptides were dried with a centrifugal adaptor and stored at -20°C until analysis by liquid chromatograph and mass spectrometry.

Proteomic data acquisition and analysis. Peptides were resuspened in 45 uL of 4% formic acid, 3% ACN, and 2uL was analyzed in on a Bruke timsTOF Pro mass spectrometry system equipped with an Bruker nanoElute high-pressure liquid chromatography system interfaced via a captiveSpray source. Samples were directly injected on a C18 reverse phase column (25 cm x 75 µm packed with ReprosilPur C18 AQ 1.9 um particles). Peptides were separated by an organic gradient from 2 to 28% ACN at 400nl/min over the course of a 120 acquisition. Each sample was injected twice,

once with data-dependent PASEF acquisition to build a spectral library, and one via a diaPASEF acquisition for quantitative analysis. The mass spectrometry data files (raw and search results) have been deposited to the Chorus project ID 1643 (www.chorusproject.org). All data-dependent PASEF files [63] were search against the Saccharomyces cerevisiae proteome database (Downloaded from the Saccharomyces Genome Database January 13, 2015). Peptide and protein identification searches were performed with the Spectronaut Pulsar software (www.spectronaut.org) to generate a spectral library of detected phosphorylated peptides with a 1% false-discovery rate at the peptide and protein level. Spectronaut was further used with the default settings to analyzed the diaPASEF data [64] and extract quantitative regulation of detected phosphorylation sites. Label-free quantification and statistical testing of phosphorylation sites was performed using the artMS R-package (version 1.3.7) (https://github.com/biodavidjm/artMS), and the MSstats statistical R-package (version 3.16.0) [65]. Instant Clue [66] was used for figure generation of proteomics data.

Spot Tests

Yeast strains were inoculated into 3-5 ml YM-1 or CSM-URA + 2% dextrose grown overnight with aeration at 30°. Fivefold dilution series were set up in 96-well plates, and 3-5 µl aliquots of the dilution series were transferred to YPD, YPGAL or CSM plates. Drug concentrations and alternative carbon sources are specified in individual figures. In experiments utilizing plasmids overexpressing *ISR1*, plates also contained 100 µg/ml NAT to maintain plasmid selection. Plates were incubated 2-3 days at 30° until colonies formed and then were photographed.

Acknowledgements

We thank Jonathan Asfaha and David Morgan for reagents and generously allowing use of their equipment. We'd also like to thank the members of the Toczyski lab for helpful discussions. This work was supported by the National Institutes of Health (R35GM118104 to DPT, R01 GM133981 to DLS).

References

1. Ptacek J, Devgan G, Michaud G, Zhu H, Zhu X, Fasolo J, et al. Global analysis of protein phosphorylation in yeast. Nature. 2005;438: 679–684. doi:10.1038/nature04187

2. Manning G, Plowman GD, Hunter T, Sudarsanam S. Evolution of protein kinase signaling from yeast to man. Trends Biochem Sci. 2002;27: 514–520. doi:10.1016/S0968-0004(02)02179-5

3. Fiedler D, Braberg H, Mehta M, Chechik G, Cagney G, Mukherjee P, et al. Functional Organization of the S. cerevisiae Phosphorylation Network. Cell. 2009;136: 952–963. doi:10.1016/j.cell.2008.12.039

4. Sharma K, D'Souza RCJ, Tyanova S, Schaab C, Wiśniewski JR, Cox J, et al. Ultradeep Human Phosphoproteome Reveals a Distinct Regulatory Nature of Tyr and Ser/Thr-Based Signaling. Cell Rep. 2014;8: 1583–1594. doi:10.1016/j.celrep.2014.07.036

5. Kannan N, Taylor SS, Zhai Y, Venter JC, Manning G. Structural and Functional Diversity of the Microbial Kinome. PLOS Biol. 2007;5: e17. doi:10.1371/journal.pbio.0050017

6. Miyahara K, Hirata D, Miyakawa T. Functional Interaction of Isr1, a Predicted Protein Kinase, with the Pkc1 Pathway in *Saccharomyces cerevisiae*. Biosci Biotechnol Biochem. 1998;62: 1376–1380. doi:10.1271/bbb.62.1376

7. Bos JL. ras Oncogenes in Human Cancer: A Review. Cancer Res. 1989;49: 4682–4689.

8. Toda T, Uno I, Ishikawa T, Powers S, Kataoka T, Broek D, et al. In yeast, RAS proteins are controlling elements of adenylate cyclase. Cell. 1985;40: 27–36. doi:10.1016/0092-8674(85)90305-8

9. Masuda T, Kariya K, Shinkai M, Okada T, Kataoka T. Protein Kinase Byr2 Is a Target of Ras1 in the Fission Yeast Schizosaccharomyces pombe. J Biol Chem. 1995;270: 1979–1982. doi:10.1074/jbc.270.5.1979

10. Scheffzek K, Grünewald P, Wohlgemuth S, Kabsch W, Tu H, Wigler M, et al. The Ras-Byr2RBD Complex: Structural Basis for Ras Effector Recognition in Yeast. Structure. 2001;9: 1043–1050. doi:10.1016/S0969-2126(01)00674-8

11. Levin DE. Regulation of Cell Wall Biogenesis in Saccharomyces cerevisiae: The Cell Wall Integrity Signaling Pathway. Genetics. 2011;189: 1145–1175. doi:10.1534/genetics.111.128264

12. Mehlgarten C, Zink S, Rutter J, Schaffrath R. Dosage suppression of the *Kluyveromyces lactis* zymocin by *Saccharomyces cerevisiae ISR1* and *UGP1*. FEMS Yeast Res. 2007;7: 722–730. doi:10.1111/j.1567-1364.2007.00216.x

13. Jablonowski D, Fichtner L, Martin VJ, Klassen R, Meinhardt F, Stark MJR, et al. Saccharomyces cerevisiae cell wall chitin, the Kluyveromyces lactis zymocin receptor. Yeast. 2001;18: 1285–1299. doi:10.1002/yea.776

14. Orlean P. Architecture and Biosynthesis of the Saccharomyces cerevisiae Cell Wall. Genetics. 2012;192: 775–818. doi:10.1534/genetics.112.144485

15. Larkin A, Imperiali B. The Expanding Horizons of Asparagine-Linked Glycosylation. Biochemistry. 2011;50: 4411–4426. doi:10.1021/bi200346n

16. Schekman R, Brawley V. Localized deposition of chitin on the yeast cell surface in response to mating pheromone. Proc Natl Acad Sci U S A. 1979;76: 645–649.

17. Lagorce A, Berre-Anton VL, Aguilar-Uscanga B, Martin-Yken H, Dagkessamanskaia A, François J. Involvement of GFA1, which encodes glutamine–fructose-6-phosphate amidotransferase, in the activation of the chitin synthesis pathway in response to cell-wall defects in Saccharomyces cerevisiae. Eur J Biochem. 2002;269: 1697–1707. doi:10.1046/j.1432-1327.2002.02814.x

18. Lesage G, Bussey H. Cell Wall Assembly in Saccharomyces cerevisiae. Microbiol Mol Biol Rev. 2006;70: 317–343. doi:10.1128/MMBR.00038-05

19. Bulik DA, Olczak M, Lucero HA, Osmond BC, Robbins PW, Specht CA. Chitin Synthesis in Saccharomyces cerevisiae in Response to Supplementation of Growth Medium with Glucosamine and Cell Wall Stress. Eukaryot Cell. 2003;2: 886–900. doi:10.1128/EC.2.5.886-900.2003

20. Valdivia RH, Schekman R. The yeasts Rho1p and Pkc1p regulate the transport of chitin synthase III (Chs3p) from internal stores to the plasma membrane. Proc Natl Acad Sci. 2003;100: 10287. doi:10.1073/pnas.1834246100

21. Milewski S. Glucosamine-6-phosphate synthase—the multi-facets enzyme. Biochim Biophys Acta BBA - Protein Struct Mol Enzymol. 2002;1597: 173–192. doi:10.1016/S0167-4838(02)00318-7

22. Milewski S, Gabriel I, Olchowy J. Enzymes of UDP-GlcNAc biosynthesis in yeast. Yeast. 2006;23: 1–14. doi:10.1002/yea.1337

23. Zibrova D, Vandermoere F, Göransson O, Peggie M, Mariño KV, Knierim A, et al. GFAT1 phosphorylation by AMPK promotes VEGF-induced angiogenesis. Biochem J. 2017;474: 983–1001. doi:10.1042/BCJ20160980

24. Chang Q, Su K, Baker JR, Yang X, Paterson AJ, Kudlow JE. Phosphorylation of Human Glutamine:Fructose-6-phosphate Amidotransferase by cAMP-dependent Protein Kinase at Serine 205 Blocks the Enzyme Activity. J Biol Chem. 2000;275: 21981–21987. doi:10.1074/jbc.M001049200

25. Graack HR, Cinque U, Kress H. Functional regulation of glutamine:fructose-6-phosphate aminotransferase 1 (GFAT1) of Drosophila melanogaster in a UDP-N-acetylglucosamine and cAMP-dependent manner. Biochem J. 2001;360: 401–412.

26. Milewski S, Kuszczak D, Jedrzejczak R, Smith RJ, Brown AJP, Gooday GW. Oligomeric Structure and Regulation of Candida albicans Glucosamine-6-phosphate Synthase. J Biol Chem. 1999;274: 4000–4008. doi:10.1074/jbc.274.7.4000

27. Zheng J, Khalil M, Cannon JF. Glc7p Protein Phosphatase Inhibits Expression of Glutamine-Fructose-6-phosphate Transaminase from GFA1. J Biol Chem. 2000;275: 18070–18078. doi:10.1074/jbc.M000918200

28. Ghaemmaghami S, Huh W-K, Bower K, Howson RW, Belle A, Dephoure N, et al. Global analysis of protein expression in yeast. Nature. 2003;425: 737–741. doi:10.1038/nature02046

29. Giaever G, Chu AM, Ni L, Connelly C, Riles L, Véronneau S, et al. Functional profiling of the Saccharomyces cerevisiae genome. Nature. 2002;418: 387–391. doi:10.1038/nature00935

30. Holbein S, Wengi A, Decourty L, Freimoser FM, Jacquier A, Dichtl B. Cordycepin interferes with 3' end formation in yeast independently of its potential to terminate RNA chain elongation. RNA. 2009;15: 837–849. doi:10.1261/rna.1458909

31. Yoo J, Mashalidis EH, Kuk ACY, Yamamoto K, Kaeser B, Ichikawa S, et al. GlcNAc-1-P-transferase-tunicamycin complex structure reveals basis for inhibition of N-glycosylation. Nat Struct Mol Biol. 2018;25: 217–224. doi:10.1038/s41594-018-0031-y

32. Ben-Shitrit T, Yosef N, Shemesh K, Sharan R, Ruppin E, Kupiec M. Systematic identification of gene annotation errors in the widely used yeast mutation collections. Nat Methods. 2012;9: 373–378. doi:10.1038/nmeth.1890

33. Barnes G, Hansen WJ, Holcomb CL, Rine J. Asparagine-linked glycosylation in Saccharomyces cerevisiae: genetic analysis of an early step. Mol Cell Biol. 1984;4: 2381–2388. doi:10.1128/MCB.4.11.2381

34. Ram AFJ, Klis FM. Identification of fungal cell wall mutants using susceptibility assays based on Calcofluor white and Congo red. Nat Protoc. 2006;1: 2253–2256. doi:10.1038/nprot.2006.397

35. Ram AFJ, Wolters A, Hoopen RT, Klis FM. A new approach for isolating cell wall mutants in Saccharomyces cerevisiae by screening for hypersensitivity to calcofluor white. Yeast. 1994;10: 1019–1030. doi:10.1002/yea.320100804

36. Roncero C, Valdivieso MH, Ribas JC, Durán A. Isolation and characterization of Saccharomyces cerevisiae mutants resistant to Calcofluor white. J Bacteriol. 1988;170: 1950–1954.

37. Sobering AK, Watanabe R, Romeo MJ, Yan BC, Specht CA, Orlean P, et al. Yeast Ras Regulates the Complex that Catalyzes the First Step in GPI-Anchor Biosynthesis at the ER. Cell. 2004;117: 637–648. doi:10.1016/j.cell.2004.05.003

38. Mitchell AP. The GLN1 Locus of SACCHAROMYCES CEREVISIAE Encodes Glutamine Synthetase. Genetics. 1985;111: 243–258. Available:

39. Watzele G, Tanner W. Cloning of the glutamine:fructose-6-phosphate amidotransferase gene from yeast. Pheromonal regulation of its transcription. J Biol Chem. 1989;264: 8753–8758.

40. Gomez A, Perez J, Reyes A, Duran A, Roncero C. Slt2 and Rim101 Contribute Independently to the Correct Assembly of the Chitin Ring at the Budding Yeast Neck in Saccharomyces cerevisiae. Eukaryot Cell. 2009;8: 1449–1459. doi:10.1128/EC.00153-09

41. Eguchi S, Oshiro N, Miyamoto T, Yoshino K, Okamoto S, Ono T, et al. AMP-activated protein kinase phosphorylates glutamine : fructose-6-phosphate amidotransferase 1 at Ser243 to modulate its enzymatic activity. Genes Cells. 2009;14: 179–189. doi:10.1111/j.1365-2443.2008.01260.x

42. Frisa PS, Sonneborn DR. Developmentally regulated interconversions between end product-inhibitable and noninhibitable forms of a first pathway-specific enzyme activity

can be mimicked in vitro by protein dephosphorylation-phosphorylation reactions. Proc Natl Acad Sci. 1982;79: 6289–6293. doi:10.1073/pnas.79.20.6289

43. Breitkreutz A, Choi H, Sharom JR, Boucher L, Neduva V, Larsen B, et al. A Global Protein Kinase and Phosphatase Interaction Network in Yeast. Science. 2010;328: 1043–1046. doi:10.1126/science.1176495

44. Holt LJ, Tuch BB, Villén J, Johnson AD, Gygi SP, Morgan DO. Global analysis of Cdk1 substrate phosphorylation sites provides insights into evolution. Science. 2009;325: 1682. doi:10.1126/science.1172867

45. Spellman PT, Sherlock G, Zhang MQ, Iyer VR, Anders K, Eisen MB, et al. Comprehensive Identification of Cell Cycle–regulated Genes of the Yeast Saccharomyces cerevisiae by Microarray Hybridization. Mol Biol Cell. 1998;9: 3273–3297. doi:10.1091/mbc.9.12.3273

46. Mark KG, Simonetta M, Maiolica A, Seller CA, Toczyski DP. Ubiquitin Ligase Trapping Identifies an SCFSaf1 Pathway Targeting Unprocessed Vacuolar/Lysosomal Proteins. Mol Cell. 2014;53: 148–161. doi:10.1016/j.molcel.2013.12.003

47. Willems AR, Schwab M, Tyers M. A hitchhiker's guide to the cullin ubiquitin ligases: SCF and its kin. Biochim Biophys Acta BBA - Mol Cell Res. 2004;1695: 133–170. doi:10.1016/j.bbamcr.2004.09.027

48. Tang X, Orlicky S, Liu Q, Willems A, Sicheri F, Tyers M. Genome-Wide Surveys for Phosphorylation-Dependent Substrates of SCF Ubiquitin Ligases. Methods in Enzymology. Academic Press; 2005. pp. 433–458. doi:10.1016/S0076-6879(05)99030-7

49. Skowyra D, Craig KL, Tyers M, Elledge SJ, Harper JW. F-Box Proteins Are Receptors that Recruit Phosphorylated Substrates to the SCF Ubiquitin-Ligase Complex. Cell. 1997;91: 209–219. doi:10.1016/S0092-8674(00)80403-1

50. Hao B, Oehlmann S, Sowa ME, Harper JW, Pavletich NP. Structure of a Fbw7-Skp1-Cyclin E Complex: Multisite-Phosphorylated Substrate Recognition by SCF Ubiquitin Ligases. Mol Cell. 2007;26: 131–143. doi:10.1016/j.molcel.2007.02.022

51. Lyons NA, Fonslow BR, Diedrich JK, Yates JR, Morgan DO. Sequential Primed Kinases Create a Damage-Responsive Phosphodegron on Eco1. Nat Struct Mol Biol. 2013;20: 194–201. doi:10.1038/nsmb.2478

52. Dephoure N, Howson RW, Blethrow JD, Shokat KM, O'Shea EK. Combining chemical genetics and proteomics to identify protein kinase substrates. Proc Natl Acad Sci. 2005;102: 17940–17945. doi:10.1073/pnas.0509080102

53. Carroll AS, Bishop AC, DeRisi JL, Shokat KM, O'Shea EK. Chemical inhibition of the Pho85 cyclin-dependent kinase reveals a role in the environmental stress response. Proc Natl Acad Sci U S A. 2001;98: 12578–12583. doi:10.1073/pnas.211195798

54. Huang D, Friesen H, Andrews B. Pho85, a multifunctional cyclin-dependent protein kinase in budding yeast. Mol Microbiol. 2007;66: 303–314. doi:10.1111/j.1365-2958.2007.05914.x

55. Espinoza FH, Ogas J, Herskowitz I, Morgan DO. Cell cycle control by a complex of the cyclin HCS26 (PCL1) and the kinase PHO85. Science. 1994;266: 1388–1391. doi:10.1126/science.7973730

56. Schneider KR, Smith RL, O'Shea EK. Phosphate-regulated inactivation of the kinase PHO80-PHO85 by the CDK inhibitor PHO81. Science. 1994;266: 122–126. doi:10.1126/science.7939631

57. Huang D, Moffat J, Wilson WA, Moore L, Cheng C, Roach PJ, et al. Cyclin Partners Determine Pho85 Protein Kinase Substrate Specificity In Vitro and In Vivo: Control of Glycogen Biosynthesis by Pcl8 and Pcl10. Mol Cell Biol. 1998;18: 3289–3299.

58. Imai K, Noda Y, Adachi H, Yoda K. A Novel Endoplasmic Reticulum Membrane Protein Rcr1 Regulates Chitin Deposition in the Cell Wall of Saccharomyces cerevisiae. J Biol Chem. 2005;280: 8275–8284. doi:10.1074/jbc.M409428200

59. Sopko R, Huang D, Preston N, Chua G, Papp B, Kafadar K, et al. Mapping Pathways and Phenotypes by Systematic Gene Overexpression. Mol Cell. 2006;21: 319–330. doi:10.1016/j.molcel.2005.12.011

60. Levin DE. Cell Wall Integrity Signaling in Saccharomyces cerevisiae. Microbiol Mol Biol Rev. 2005;69: 262–291. doi:10.1128/MMBR.69.2.262-291.2005

61. Bandyopadhyay S, Mehta M, Kuo D, Sung M-K, Chuang R, Jaehnig EJ, et al. Rewiring of Genetic Networks in Response to DNA Damage. Science. 2010;330: 1385–1389. doi:10.1126/science.1195618

62. Costanzo M, VanderSluis B, Koch EN, Baryshnikova A, Pons C, Tan G, et al. A global genetic interaction network maps a wiring diagram of cellular function. Science. 2016;353: aaf1420. doi:10.1126/science.aaf1420

63. Meier F, Brunner A-D, Koch S, Koch H, Lubeck M, Krause M, et al. Online Parallel Accumulation–Serial Fragmentation (PASEF) with a Novel Trapped Ion Mobility Mass Spectrometer. Mol Cell Proteomics MCP. 2018;17: 2534–2545. doi:10.1074/mcp.TIR118.000900

64. Meier F, Brunner A-D, Frank M, Ha A, Voytik E, Kaspar-Schoenefeld S, et al. Parallel accumulation – serial fragmentation combined with data-independent acquisition (diaPASEF): Bottom-up proteomics with near optimal ion usage. bioRxiv. 2019; 656207. doi:10.1101/656207

65. Choi M, Chang C-Y, Clough T, Broudy D, Killeen T, MacLean B, et al. MSstats: an R package for statistical analysis of quantitative mass spectrometry-based proteomic experiments. Bioinforma Oxf Engl. 2014;30: 2524–2526. doi:10.1093/bioinformatics/btu305

66. Nolte H, MacVicar TD, Tellkamp F, Krüger M. Instant Clue: A Software Suite for Interactive Data Visualization and Analysis. Sci Rep. 2018;8. doi:10.1038/s41598-018-31154-6

Publishing Agreement

It is the policy of the University to encourage open access and broad distribution of all theses, dissertations, and manuscripts. The Graduate Division will facilitate the distribution of UCSF theses, dissertations, and manuscripts to the UCSF Library for open access and distribution. UCSF will make such theses, dissertations, and manuscripts accessible to the public and will take reasonable steps to preserve these works in perpetuity.

I hereby grant the non-exclusive, perpetual right to The Regents of the University of California to reproduce, publicly display, distribute, preserve, and publish copies of my thesis, dissertation, or manuscript in any form or media, now existing or later derived, including access online for teaching, research, and public service purposes.

DocuSigned by:
Emma B Allme
6A94BBA7BC32415...
Author Signature

2/19/2020
Date